Synthesis and Crystal Chemistry of Bimetallic Group II Nitride Fluorides

By

Jersfrey Omwenga Omwenga

Submitted in Partial Fulfillment of the Requirements

For the Degree of

Master of Science

in the

Chemistry

Program

YOUNGSTOWN STATE UNIVERSITY

August, 2018

Synthesis and Crystal Chemistry of Bimetallic Group II Nitride Fluorides

By

Jersfrey Omwenga Omwenga

I hereby release this thesis to the public. I understand that this thesis will be made available from the Ohio LINK ETD Center and the Maag Library Circulation Desk for public access. I also authorize the University or other individuals to make copies of this thesis as needed for scholarly research.

Signature:

_____

Jersfrey Omwenga Omwenga, Student Date

Approvals:

_____

Dr. Timothy R. Wagner, Thesis Advisor Date

_____

Dr. Sherri Lovelace-Cameron, Committee Member Date

_____

Dr. Christopher Arntsen, Committee Member Date

_____

Dr. Salvatore A. Sanders, Date
Dean, College of Graduate Studies

ABSTRACT

This thesis project focused on the synthesis and crystal chemical characterization of single crystalline bimetallic nitride fluorides of general composition BaMNF, with M = Mg, Sr, & Ca. Single crystalline samples were grown through slow cooling of metal and metal fluoride mixtures reacted under nitrogen gas at high temperature. High resolution X-ray diffraction data was collected and used to elucidate the crystal chemistries of the new phases, which are described in detail. Compositional analysis using energy dispersive spectroscopy combined with the FIB (Focused Ion Beam) milling technique in a scanning electron microscope was performed on two phases, possibly indicating small amounts of oxygen contamination in these compounds.

Four new Group II bimetallic nitride fluoride phases were prepared and characterized via single crystal X-ray diffraction in this study. A Sr-rich BaSrNF ordered rocksalt-type phase was prepared showing some disorder and a non-stoichiometric defect. BaSrNF (Sr-rich) and BaCaNF (Ba-rich) disordered rocksalt-type compounds were prepared. A Ba-rich BaCaNF rhombohedral phase was also prepared and characterized, and crystal chemical factors governing the choice of rhombohedral vs. the ordered rocksalt-type cubic structure are discussed. Attempts to prepare BaMgNF compounds were unsuccessful. Finally, previous studies were revisited on Sr_2NF to further elucidate the crystal chemistry of this phase as a baseline for BaSrNF studies. No Group II bimetallic inorganic nitride fluoride compounds have been previously reported in the literature. Such bimetallic compounds could offer the ability to tune band-gaps and thus optical and electronic properties relative to single metal M_2NF compounds.

ACKNOWLEDGEMENTS

First and above all, I thank God for providing me with this opportunity and enabling me to complete this project successfully through his blessings.

I would like to thank my advisor Dr. Tim Wagner for the support that he has given me during the two year period while I was working in his lab. It's my desire to be as calm, patient and motivating as my advisor has been for the period I have worked with him. Dr.Wagner has provided discerning discussions more specifically on this research project. The scientific advice, knowledge, suggestions and discussions provided me with logical answers to the many questions which were vital in handling the whole research work.

I also have to thank members of my masters committee Dr. Sherri Lovelace Cameron and Dr. Christopher Arntsen for agreeing to be a part of the committee and to contribute for the overall success of this project. I thank Raymond E. Hoff for instrumental analysis guidance and training and Tim Styranec for laboratory safety training and ensuring that there was no shortage in terms of chemical supplies.
My sincere recognition goes to the Youngstown State University and more specific to the chemistry department for the admission, financial support and guidance throughout the program.

Special mention to my lovely wife Steficah for her unwavering support and love, my mum and my sisters for all they have been to me. I dedicate this thesis to them as a way of showing my appreciation.

TABLE OF CONTENTS

LIST OF FIGURES

FIGURE

LIST OF TABLES

TABLE

LIST OF REACTIONS

CHAPTER ONE

INTRODUCTION TO INORGANIC NITRIDE FLUORIDES COMPOUNDS

1.1 Introduction

This particular area of inorganic chemistry still has a lot of research work to be done since relatively few nitride fluoride compounds have been synthesized successfully so far. Most of the nitride fluoride compounds synthesized are considered pseudo oxides, where N^{3-} (nitride) and F^{-} (fluoride) ions replace two O^{2-} anions in an oxide analog ($2O^{2-} \rightarrow N^{3-} + F^{-}$), an example is Mg_2NF which is an analog of MgO. Relative to the oxides, nitride fluoride compounds display a rich crystal chemistry, due largely to various possibilities for ordering of N^{3-} and F^{-} ions.

1.2 Single-metal nitride fluoride: Alkaline earth metals

Andersson (1970) was one of the earliest researchers who reported a study on nitride-fluoride compounds, focusing on magnesium nitride fluorides. The researcher used powder X-ray diffraction to deduce three phases whose structures were related to MgO rocksalt-type. Mg_3NF_3 has a cubic phase with space group $Pm\bar{3}m$, which showed ordering of N^{3-} and F^{-} with one-fourth of Mg^{2+} sites vacant are empty. The Mg^{2+} ions are coordinated octahedrally at equal distances of 2.108 Å to four fluoride and two nitride ions.

A second phase, L-Mg_2NF (low temperature polymorph) was indexed as tetragonal and thus considered to take an *anti* –$LiFeO_2$ type structure, where F^{-} occupies the corresponding Fe^{3+} position, N^{3-} occupies the Li^{+} position and Mg^{2+} is positioned on the homologous anion (O^{2-}) position. It has ordered anions causing the doubling along one of the dimensions of MgO cubic structure. L-MgNF has $I4_1/amd$ space group, where

a = 4.186 Å, c = 10.042 Å. This was described as an intermediate between sodium chloride and zinc blende structures which form a square pyramid when magnesium is coordinated to three nitrogen and two fluorine atoms. A third phase, H-Mg_2NF (high temperature polymorph) is cubic with disordered N^{3-} and F^- anions. The L-Mg_2NF is reacted at high temperature (1100-1350°C) and pressure (25-30 kbar) and the argon treatment at 900°C transforms to H-Mg_2NF.Ehrlich *et al*. (1971) later worked on the three alkali earth metals which included: calcium, strontium and barium nitride fluorides (M_2NF where M = Ca or Sr or Ba) The reaction synthesis was carried out in an inert atmosphere (argon) for 24 hours at 1000°C and then switched to nitrogen gas for 24 hours for calcium, strontium and barium at 1000°C, 950°C and 700°C, respectively. The strontium and barium nitride fluoride reactants had similar stoichiometric ratios of metal to metal fluoride of 3:1, while for the Ca_2NF reaction, the metal to metal fluoride stoichiometric ratio was 4:1. The reactants were also heated to high temperatures of up to a 1000°C for 24 hours under nitrogen gas flow. Characterization of the final chemical compounds produced utilized the Debye-Scherrer powder X-ray diffraction where it suggested the presence of two phases, MF_2 and M_2NF. These phases were analogous to their metal oxides through the similar rocksalt structures.

Brogan *et al.* (2012) prepared and analyzed three phases of a magnesium nitride compound which included Mg_3NF_3 and L-Mg_2NF using the standard ceramic reaction methods. The authors characterized the products using the powder X-ray and powder neutron diffraction techniques. Mg_3NF_3 was synthesized using temperatures of up to 1323 K. Indexing of its peaks gave a unit cell length of 4.2153Å which was in agreement with Andersson's value of 4.216 Å. Mg_3NF_3 is cubic with $Pm\bar{3}m$ space group and its

structure is analogously to MgO, but with one cation site vacant. Mg is located on the 3c (0, 1/2, 1/2) site and with the vacant (0, 0, 0) site an octahedral magnesium connected to two nitride and four fluoride anions. The synthesis of L-Mg_2NF was heated up to 1423 K as the maximum temperature. Indexing of peaks suggested a tetragonal unit cell whose space group was $I4_1/amd$ with a = 4.1816 Å and c = 10.0322(6) ˚A which compared closely with previously reported literature data (Andersson, 1970) values of a = 4.186 Å and c = 10.042 Å. The compounds they also both form structures possessing crystallographically ordered nitride and fluoride anions.

Galy *et al*. (1971) previously reported that a Ca_2NF phase prepared in a solid state stoichiometric reaction mixture of Ca_3N_2 and CaF_2 for 24 hours at 900 °C had rocksalt type structure with unit cell parameter a = 4.965 Å. The authors also concluded that the unit cell parameter increases as x decreases in $Ca_2N_{1-x}O_{2x}F_{1-x}$, that is, as the nitrogen content increases.

More recently, Strozewski (2007) reported a rocksalt-type structure after preparing a Ca-N-O-F sample by a stoichiometric reaction of CaO and CaF_2 with Ca metal in nitrogen atmosphere. This phase was analyzed via single crystal X-ray diffraction at room temperature, and the unit cell parameter was found to be a = 4.937 Å. This is identical to the cell parameter reported by Ehrlich *et al*. (1971) for their Ca_2NF sample, suggesting that this may actually be a Ca-N-O-F phase. **Figure 1.1** shows a structure plot from single crystal X-ray diffraction analysis for a Ca_2NF-type rocksalt phase prepared by Strozewski (2007), having a = 4.986 Å. This value is somewhat higher than the values reported by both Ehrlich et al. (1971) and Galy (1971) for their Ca_2NF samples, suggesting that Strozewski's sample has higher N-F content.

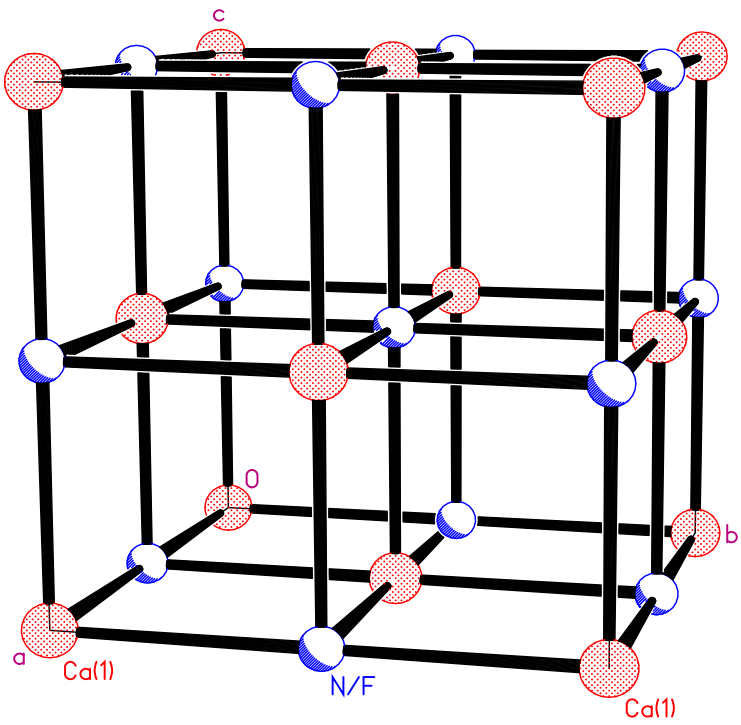

Figure 1.1. A structural rocksalt type Ca_2NF (Strowzeski, 2007) plot from single crystal X-ray diffraction data.

Nicklow *et al*. (2001) previously reported the synthesis of single crystalline Ca_2NF prepared in a 3:1 mole ratio of Ca: CaF_2 reacting under nitrogen gas at 1000 °C. The Ca_2NF phase reported has a tetragonal unit cell with space group I41/amd and a = 4.901 Å, c = 10.516 Å. The authors concluded that the Ca_2NF compound was isostructural with the L-Mg_2NF reported earlier by Andersson (1970) since the parameters are similar. Jack *et al*. (2005) reported yet another Ca_2NF phase which is isostructural to an ordered rocksalt (also referred to as doubled cubic) Sr_2NF phase (see below) reported by Wagner (2002), having a space group of $Fd\bar{3}m$ and a unit cell parameter a = 10.0215(8) Å. The N and F atoms show ordering along all the three cell directions. Optimal refinement of the

single crystal X-ray data for Ca_2NF required positioning of F atoms on the tetrahedral interstitial lattice sites, modeled as a Frenkel defect. Note that the calcium nitride fluoride system has been reported in all the three phases discussed so far (rocksalt, L-Ca_2NF, and doubled cubic phases), whereas other alkaline earth metals have only crystallized in one or two of the phases.

Wagner (2002) prepared single crystals of Sr_2NF which were cubic with space group $Fd\bar{3}m$ but with unit cells doubled along all the three axes in relation to the Sr_2NF rocksalt type. These crystals were synthesized by heating Sr metal and SrF_2 in a mole ratio of 3:1 to a melt up to 1000ºC under a continuous flow of nitrogen gas. As mentioned, this structure is due to ordering of N and F atoms along all three unit cell axes. Two different colors of doubled cubic Sr_2NF crystals were reported: brownish yellow with unit cell parameter a = 10.6920 (45) Å; and dark red crystals with a = 10.7655 (20) Å. During refinement, residual electron density was observed in the interstitial tetrahedral sites of the lattice, which was determined to be due to the presence of F atoms. This was modeled as a Frenkel defect, with F atoms moving from the normal octahedral F1 positions to the interstitial sites.

Al-Azzawi *et al*. (2017) recently reported the synthesis and structure analysis of doubled cubic Ca_2NF using high resolution x-ray diffraction data, and discovered that the interstitial fluoride ions previously interpreted as Frenkel defects are actually due to non-stoichiometric defect with excess fluorine present. The F1 octahedral positions are fully occupied and are disordered, splitting into F1B positions 0.575 Å on either side of the F1 site depending upon occupancy of

the nearby F2 interstitial position. The X-ray structure plot for doubled cubic Ca_2NF reported by Al-Azzawi is shown in **Figure 1.2,** and a coordination sphere for Ca is shown in **Figure 1.3.** A similar structure was observed for Sr2NF in this work, as discussed later in Chapter 6.

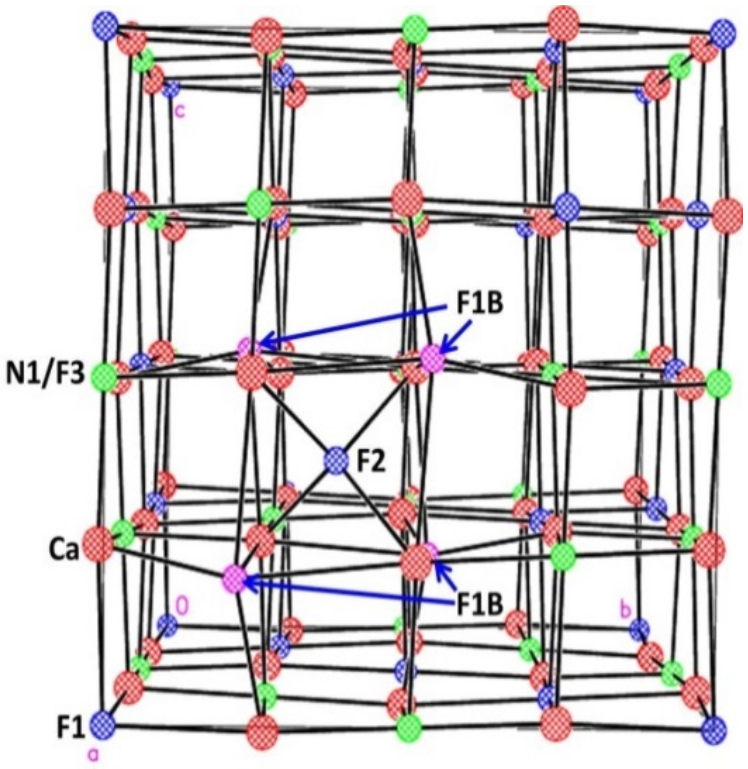

Figure 1.2. Ca_2NF unit cell structure by Al-Azzawi *et al*. (2017) indicating the ordering of N and F atoms along the axes. One F2 interstitial position is shown; there are 1.7 interstitial atoms per unit cell. Also evident is disorder at the F1 octahedral sites, which split into F1B atoms on either side of F1 octahedral sites.

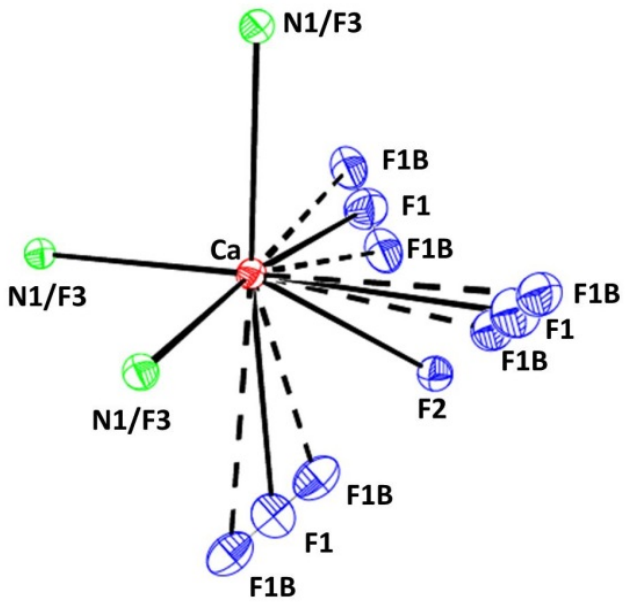

Figure 1.3. Coordination environment of a Ca atom in doubled cubic Ca_2NF showing how F1 atoms split into F1B positions to increase the distance from nearby F2 atoms. 75% ellipsoids. Al-Azzawi *et al*. (2017).

Siebel and Wagner (2004) previously reported the synthesis of Ba_2NF where the mixture was heated to 900 °C with a continuous flow of nitrogen gas. The mixture had a mole ratio of 3:1 of Ba to KCuF3, this was placed in a silica tube for reaction. The final products had very small and highly air sensitive dark violet crystals of Ba_2NF. X-ray diffraction data indicated cell parameters of a = 5.6796 (19) Å and space group $Fm\bar{3}m$. This Ba_2NF phase was reported to be isostructural with rocksalt type BaO. The cell parameter (a = 5.6796 Å) is very close to the value recorded by Ehrlich *et al*. (1971) of a = 5.691 Å.

Bailey *et al*. (2011) synthesized Ba_2NF in a 2:1 mole ratio of Ba_2N to BaX_2 (where X = F, Cl or Br) under argon atmosphere at 998 K for five days. The reactions led

to the formation of black/grey products of Ba_2NF. Characterization data from the powder X-ray diffractometer revealed the presence of two phases: one that is cubic with a space group of $Fm\bar{3}m$, and another that is hexagonal with a = 4.0242 (5) c = 19.975 (2) Å in space group $R\bar{3}m$ similar to the anti-α-$NaFeO_2$ structure also adopted by other alkaline earth nitride halides. The authors noted this to be the first nitride fluoride compound to crystallize in a layered hexagonal system.

Synthesis and characterization of alkaline earth nitride fluorides has yielded a number of phases (M_2NF where M = Mg, Ca, Sr and Ba) which are outlined in **Table 1.1** below.

Table 1.1 Summary of metal nitride fluoride compounds previously prepared

Oxide Analog (Rocksalt)	**Metal Nitride Fluoride**			
	Tetragonal	**Layered Hexagonal**	**Rocksalt**	**Ordered Rocksalt (Doubled Cubic)**
MgO	[a, b] L-Mg_2NF		[a] H-Mg_2NF	
CaO	[c] L-Ca_2NF		[e, f] Ca_2NF	[h] Ca_2NF
SrO			[e, k] Sr_2NF	[l] Sr_2NF
BaO		[d] Ba_2NF	[d, e, g] Ba_2NF	

[a] Andersson, (1970); [b] Brogan *et al*., (2012); [c] Nicklow *et al*.; (2001); [d] Bailey *et al*., (2011); [e] Ehrlich *et al*., (1971); [f] Strozewski, (2007); [g] Seibel & Wagner, (2004); [h] Jack *et al*., (2005); [i] Wagner, (2002); [j] Al-Azzawi, (2016); [k] Keino (2017).

1.3 Bimetallic nitride fluorides

Relatively few bimetallic nitride fluoride compounds have been successfully prepared and reported. Headspith *et al*. (2009) prepared $CeMnN_3F_{2-d}$ from ternary nitride via fluorine insertion using fluorine gas. The synthesis of $CeMnN_3F_{2-d}$ was carried out at low temperatures between 95-115 ºC. A tetragonal symmetry with space group P4/nmm and unit cell parameters a = 3.8554(4) Å) and c = 13.088(4) Å were found on the $Ce_2MnN_3F_{2-d}$ fluorinated phase using the neutron powder diffractometer. A fluorine deficiency was revealed from the neutron powder diffraction data. Manganese ions are located in the distorted MnN_5F octahedral with manganese moved approximately 0.4 Å from its ideal unit cell position. The ordering of N and F at the octahedral apical sites along the c-axis of the unit cell causes the asymmetric surrounding for manganese.

A phase of metastable Na_xZrNF_{1+x} (x=0.3) was synthesized by Stoltz *et al*. (2005) where recrystallized β-ZrNCl was reacted with excess NaF at 350-400ºC in vacuo for ten days along intermediate grinding. X-ray and neutron diffraction data were obtained to determine the phase's structure. A number of models refined to one among the three space groups $P6_3/mmc$, $R\bar{3}m$, and $P\bar{3}m$with $P6_3/mmc$ singled out as the best. The ideal structural model is related to the layered ZrNCl-type of structure which has sequential two layer repeat unit of $F\text{-}Zr_2N_{2\text{-}F}$ against β –ZnNCl which is a three layered repeat unit. An inter-layer of sodium ad fluorine atoms located between $F\text{-}Zr_2N_2\text{-}F$ layers show partial occupancies and disorder with sodium atoms situated in pseudo octahedral sites. All these layers produce a double layer hexagonal lattice which has unit cell parameters a = 3.660(4) Å and c = 18.14(2) Å.

CaMgNF and SrCaNF bimetallic compounds were reported in MS theses by Al-Azzawi (2016) and Keino (2017), respectively, Al-Azzawi reported a CaMgNF quadrupled phase, while Keino reported a SrCaNF ordered rocksalt phase. While the CaMgNF crystal was not of high enough quality for complete structure refinement, the unit cell (a = 20.8074(57) Å) was taken as correct. SrCaNF was of high quality, and the structure is shown in **Figure 1.3**. Refined occupancies revealed excess fluorine in the lattice, with overall composition $Sr_{1.03}Ca_{0.97}N_{0.94}F_{1.17}$ relative to ideal formula of SrCaNF.

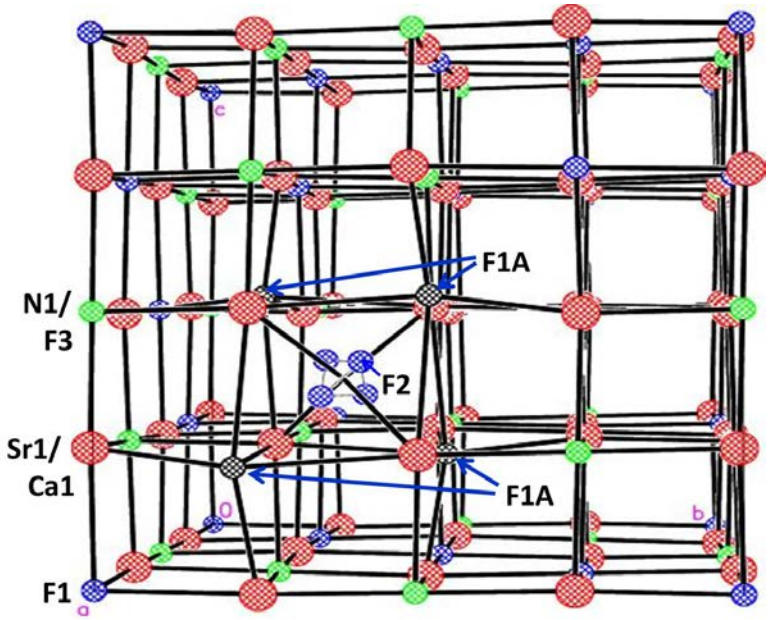

Figure 1.4. SrCaNF unit cell plot (Z = 16) showing a disordered interstitial F2 atom (Keino, 2017).

Displacement of atoms from normal F1 octahedral positions to crystallographically equivalent F1A positions on either side of F1 occurs likely due to the presence of nearby interstitial F2 atoms (2.94 per unit cell), as discussed above for Ca_2NF. For SrCaNF, there is further disorder at the F2 position, as evident in Figure 1.3. Here, F2 atoms are displaced from the tetrahedral position to one of four

crystallographically equivalent sites surrounding the tetrahedral lattice position. Although there is excess F in the lattice overall, the refined occupancies revealed that approximately one F1 site is vacant per unit cell. The shift in F2 position is likely therefore towards a vacant F1 site. In addition, Sr and Ca atoms are on slightly different postions located only 0.14 Å distance apart.

CHAPTER TWO

STATEMENT OF THE PROBLEM

Solid state inorganic nitride fluoride chemistry remains largely unexplored relative to oxides. While thousands of inorganic oxides have been synthesized and characterized, fewer than fifty nitride-fluoride compounds can be found in the literature, and many of these are poorly characterized. Perhaps the most studied are the Group II M_2NF compounds, with M = Mg, Ca, Sr & Ba. In particular, M_2NF phases analogous to MO rocksalt-type oxides have been known for some time. Other phases more recently discovered, such as ordered rocksalts, show a very rich crystal chemistry relative to the oxides due to ordering of N and F atoms in the lattice that is combined with various types of local disorder. Besides crystal chemistry effects, the optical and electronic properties of nitride fluorides relative to the analogous oxides are also often enhanced. The presence of nitrogen decreases the band gap relative to the oxide in the solid, so that while Group II MO compounds are colorless insulators, M_2NF phases have color and are semi-conductors.

Of the inorganic nitride-fluorides that have been studied, only two bimetallic phases have been reported in the literature, neither of which includes Group II metals. In this thesis, new bimetallic nitride-fluoride N-F phases in the systems BaMNF (M = Mg, Ca, and Sr) will be synthesized via standard ceramic methods (mixture of simple precursors) and characterized mainly via single crystal X-ray diffraction methods. Although band gaps will not be measured in this work, it is expected that mixed metal compositions could be a way to tune band gaps relative to M_2NF phases. Focus here will

be on elucidating the crystal chemistry of the compounds prepared. Of interest is whether or not new phases will be discovered with cation ordering in the lattice.

In addition to the bimetallic phases mentioned above, a second objective of this thesis work is to more thoroughly characterize the crystal chemistry of ordered rocksalt-type Sr_2NF, utilizing the new high resolution X-ray diffractometer available for this study. Recent work that has elucidated the crystal chemistries of ordered rocksalt-type Ca_2NF and Ba_2NF (which forms a layered rhombohedral structure) phase are available. These phases will serve as a baseline to aid in understanding the crystal chemistries of some of the Group II bimetallic phases to be prepared in this work.

CHAPTER THREE

METHODOLOGY AND EQUIPMENT

3.1 Synthetic Methods

Syntheses experiments in this thesis were performed using a standard ceramic method approach. This technique involves heating stoichiometric mixtures of simple starting materials in the solid state to high temperatures (~900-1600 ºC). The classic standard methods procedure for the preparation of Group II inorganic nitride-fluorides would be to react the M_3N_2 nitride with MF_2 to give M_2NF. This reaction would occur in the solid state and yield a powder product. For this thesis work, characterization of the crystal chemistry of the new compounds is better achieved using single crystalline samples. These will be prepared by reacting the Group II metals with metal fluorides N2. For example, for the preparation of the phase BaSrNF, the reaction is:

$$SrF_2 + Sr + 2Ba + N_2 \rightarrow 2\ BaSrNF$$

The mixture is melted by heating to high temperature and slowly cooled down to enhance growth of crystals.

Care must be taken to keep air and moisture out of the reaction systems, as this is crucial to the successful preparation of N-F compounds. The Group II nitride fluorides react quickly with water in air to release ammonia. For example:

$$2\ M_2NF + 6\ H_2O \rightarrow 3\ M(OH)_2 + MF_2 + 2\ NH_3$$

Air sensitive techniques used in this study are discussed below.

3.2 Equipment

The project involved using air and moisture sensitive solid starting materials to produce target products that are also air sensitive. Use of a glove bag under an inert Ar environment was suitable to prevent any contamination to the materials. The glove bag was connected directly to the reaction tube in the furnace for direct transport of reactants into the tube while under inert atmosphere. The Inconel reaction tube was sealed from air during the reaction. Use of a glove bag, flow of dry, high purity (99.9999%) Ar or N_2 gas throughout the treatment process, and mineral oil during crystal selection all focused to protect the materials from air.

3.2.1 Glove Bag

A glove bag is a basic technique to dispense and maintain an inert environment in a chemical manipulation process. This is done in an enclosed transparent polyethylene bag with a positive supply of pressure of an inert gas. The bag is designed with inward pointing gloves to enable the handling of materials inside the bag. A gas inlet tube is inserted into the small opening at the top of the bag and sealed with a rubber band.

The front flap enables the operator to insert materials and the bag is purged in an inflating and deflating sequence of the bag. Zipper lock is used to seal the flap and the gas flow is regulated to maintain the bag in an inflated state, this is shown in **Figure 3.1** below. Manipulations within the glove bag are facilitated by the presence of inward pointing gloves. Sensitive solid starting materials are not contaminated within the glove bag due to inert atmosphere.

Figure 3.1. A polyethylene glove bag used for solid starting materials and product preparations.

3.2.2 Tube Furnace

A programmable tube furnace is connected with a long cylindrical tube and is used for carrying out reactions at high but controlled temperatures. Samples inside a nickel crucible are placed on a nickel metal boat under inert atmosphere in the glove bag and inserted into the tube using a long push rod. The tube serves as a heating section which is encompassed by the heating elements and thermal insulation. It has two openings which serve as insertion point where solid starting materials are inserted into the tube and a capped end where the gases evolved escape into the bubbler. The bubbler monitors the gas flow rate as the reaction is ongoing. For this work three different tube furnaces were used: Thermolyne 59300, Lindberg and Mellen NACCI series 3x-12. They were typically operated at high temperatures between 900-1200°C, although the maximum operation temperatures of these furnace is 1700°C, 1500°C, and 1200°C, respectively. The main gases used were argon and nitrogen for the whole temperature treatment.

Figure 3.2. The programmable Lindberg tube furnace used for some of the high temperature reactions under argon or nitrogen gas in this work.

CHAPTER FOUR

CHARACTERIZATION METHODS

4.1 Single Crystal X-ray Diffraction

Single crystal X-ray diffraction was utilized to determine the crystal structures of the synthesized products. The Bruker D8 QUEST was the only instrument used among the three single crystal diffractometers available in YSU X-ray lab for this project. This is due to its high resolution and variable temperature (Oxford cryostream 700 plus, 80-500 K) capabilities. It is also set up with a very high brightness Molybdenum IμS Incoatec micro source; 100 cm2 Photon 100 Complementary Metal Oxide Sensor detector; Helios optics and kappa 4-axis goiniostat.

A new CMOS technology feature facilitates the detector data collection speed while the keeping the shutter uninterruptedly open for the whole collection period. The low temperature capability and the presence of nitrogen gas flow during the data collection process in the X-ray diffractometer kept our compounds from decomposing in air during the data collections.

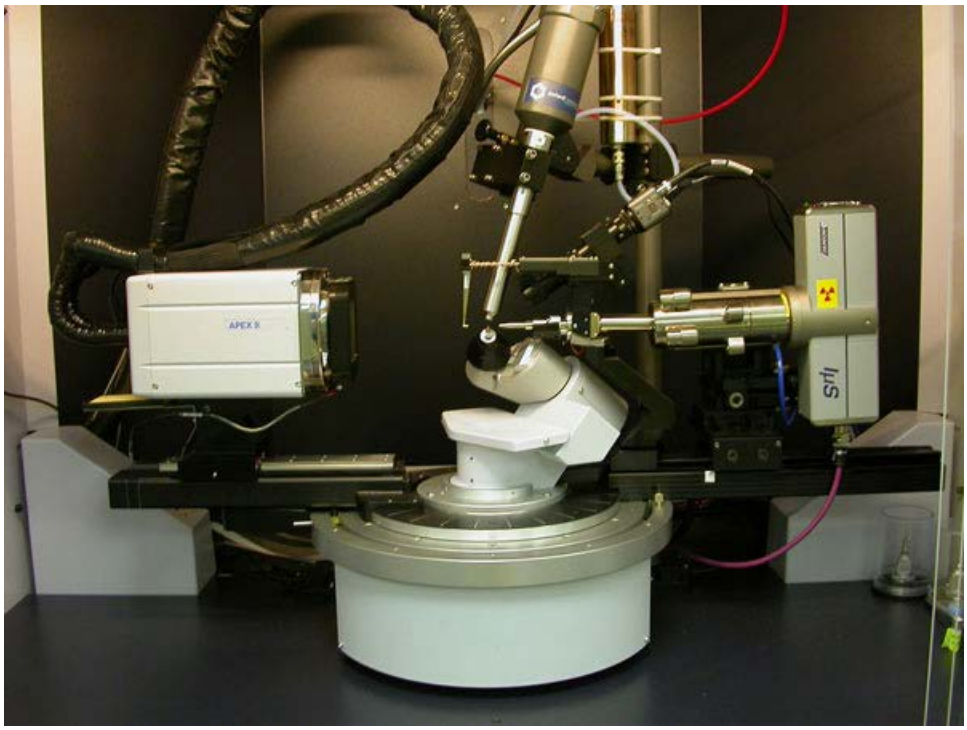

Figure 4.1. YSU single-crystal X-ray diffraction, Bruker Quest instrument used in this research.

Structure solution and refinement of our compounds was done using the SHELXTL (Sheldrick, 2008) suite of programs. SHELXTL refines experimental data from the X-ray diffractometer to realize a sensible chemical structure. A CIF file generated at the end of structure solution provides crystal information such as atom positions, types of atoms, bond lengths and bond angles. CIF file produced is in a crystallographically accepted format, allows one to check on regression factors and goodness of fit limits.

4.2 Focused Ion Beam/Scanning Electron Microscopy

A JEOL JIB-4500 Focused Ion Beam (FIB)/Scanning Electron Microscope (SEM) set up with an EDAX Apollo XV Energy-Dispersive Spectrometer is available in the YSU Electron Microscopy facility. It was utilized for compositional analysis of the compounds synthesized. The FIB/SEM sections include a vacuum column, a metal ion source, a sample holder and a detector. Ion beams (usually gallium) are used in the FIB technique and it can be operated at high or low current beam. A vacuum column has a set of apertures and lenses where the ion beam goes through to strike the sample surface to generate species like sputtered atoms, secondary electrons and secondary ions. An image of the sample is produced after ions generated are collected by the detector. Additionally this technique has a capability of cutting cross sections, observe elemental and phase compositional maps and also etching.

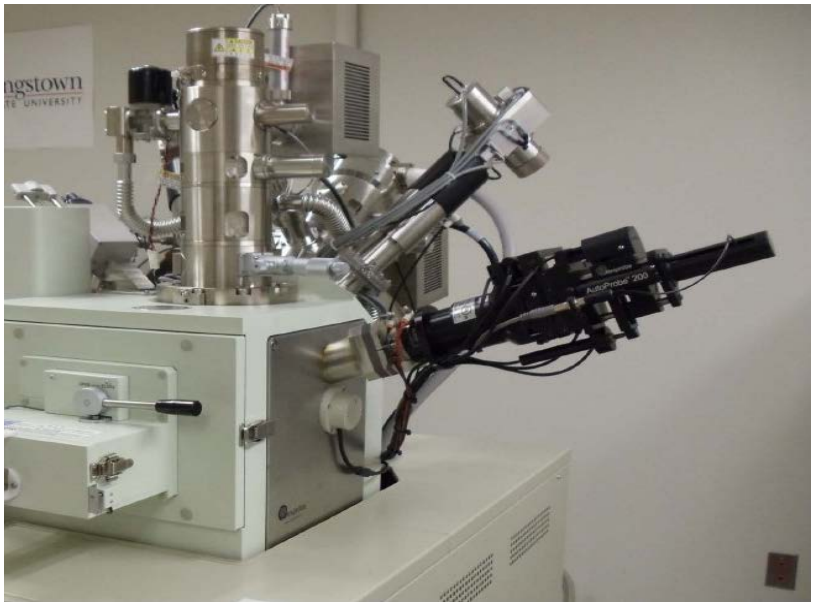

Figure 4.2. JEOL JIB-4500 Multi-beam System (SEM/FIB) used in compositional analysis of this project.

CHAPTER FIVE

CRYSTAL CHEMISTRY OF ORDERED ROCKSALT-TYPE Sr_2NF

5.1 Preparation of Sr_2NF single crystals

The purpose of this synthesis was to remake Sr_2NF to better quantify the crystal chemistry of the ordered rocksalt-type phase utilizing the new high resolution single X-ray diffractometer (see Chapter2) now available for the study. The previous work on Sr_2NF by Wagner (2002) described in Section 1.2 showed a Frenkel defect involving F atoms and large displacement of the F atoms located at normal octahedral lattice positions.

Sr_2NF was thermally treated to 1000ºC and the melting points for the reactants were 777ºC for strontium and 1477ºC for strontium fluoride. The mixture of 2.5 g of Sr metal (Alfa Aesar 98.8%) and 1.2 g SrF_2 was carried out in an Ar-filled glove bag. These two starting materials were weighed and loaded into a nickel crucible, and then inserted into the Inconel tube from the glove bag. The following reaction was used in preparing single crystals of Sr_2NF:

$$3Sr + SrF_2 + N_2 \rightarrow 2Sr_2NF$$

The mixture was heated first under an argon flow and then followed by a nitrogen flow using the following program (R = Ramp function, L = Temperature level, and D = Dwell time):

Step 1:	R1	Step Function	L1	100ºC	D1 0 Hours
Step 2:	R2	60ºC /hr.	L2	1000ºC	D2 1 Hours

Step 3: R3 100ºC /hr. L3 200ºC D3 4 Hours

Step 4: R4 60ºC /hr. L4 1000ºC D4 4 Hours

Step 5: R5 15ºC /hr. L5 200ºC D5 0 Hours

Step 6: R6 Step Function L6 80ºC D6 0 Hours

Step 7: End

The switch of gases from argon to nitrogen flow was performed in dwell three. With the seven steps followed, the cycle was completed, the nitrogen gas flow was discontinued and the furnace was switched off to cool down. The nickel crucible was removed from the Inconel tube and transferred into an argon filled glove bag. A glass slide containing a drop of mineral oil was used to place a fraction of the sample in the nickel crucible. The mineral oil enables easier handling while selecting crystals and increases the lifetime of crystals to prevent them from decomposing down. The sample on the slide was observed under an optical microscope for selection and isolation of a single crystal for analysis in the single X-ray diffractometer. The product mixture contained yellow crystals with a few black chunks, presumably a nitride phase. Black particles embedded in the single crystal were selected for analysis also. A yellow crystal of dimensions $0.207 \times 0.382 \times 0.415$ mm^3 was selected for X-ray analysis.

5.2 Single Crystal X-ray Data Collection

The Bruker D8 QUEST single crystal diffractometer described in Section 4.1 was used to perform the X-ray diffraction experiment. The unit cell was determined from

2083 reflections using the program *Cell Now* called from Bruker's APEX3 program. Of these, 1,984 reflections were exclusively indexed to the cubic unit cell with a = 10.6729(3) Å, the remaining 99 were not assigned to a domain. A half-sphere of intensity data was collected to a resolution of 0.45 Å.

5.3 Compositional analysis

Compositional analysis was conducted using the dual Focused Ion Beam (FIB)/Scanning Electron Microscope (SEM) equipped with an EDAX Apollo XV EDXS system described in Section 4.2. The main purpose of the FIB/EDAX analysis was to check for the presence of oxygen on both the surface and at the core of the crystal mounted on the diffractometer. The analysis involved surface observation and then core observation where layers were milled away using the focused ion gallium beam to be able to reach the inner core.

The data is shown in **Figure 5.1** indicating that oxygen was detected on both surface and core levels, suggesting a possible contamination of the crystal. With several core sampling regions analyzed, the presence of oxygen still was observed for both surface levels. The data does show that the inner core has a significantly reduced percentage of oxygen relative to the crystal surface, indicating that crystal decomposition did likely occur during transport of the crystal from the X-ray diffractometer to the adjacent electron microscopy lab. Of course, this does not prove the complete absence of oxygen before decomposition began. It should also be noted that we could not be sure that surface debris from milling did not contaminate the core during EDS analysis. Refinement of the structure with oxygen present showed very slightly poorer R values

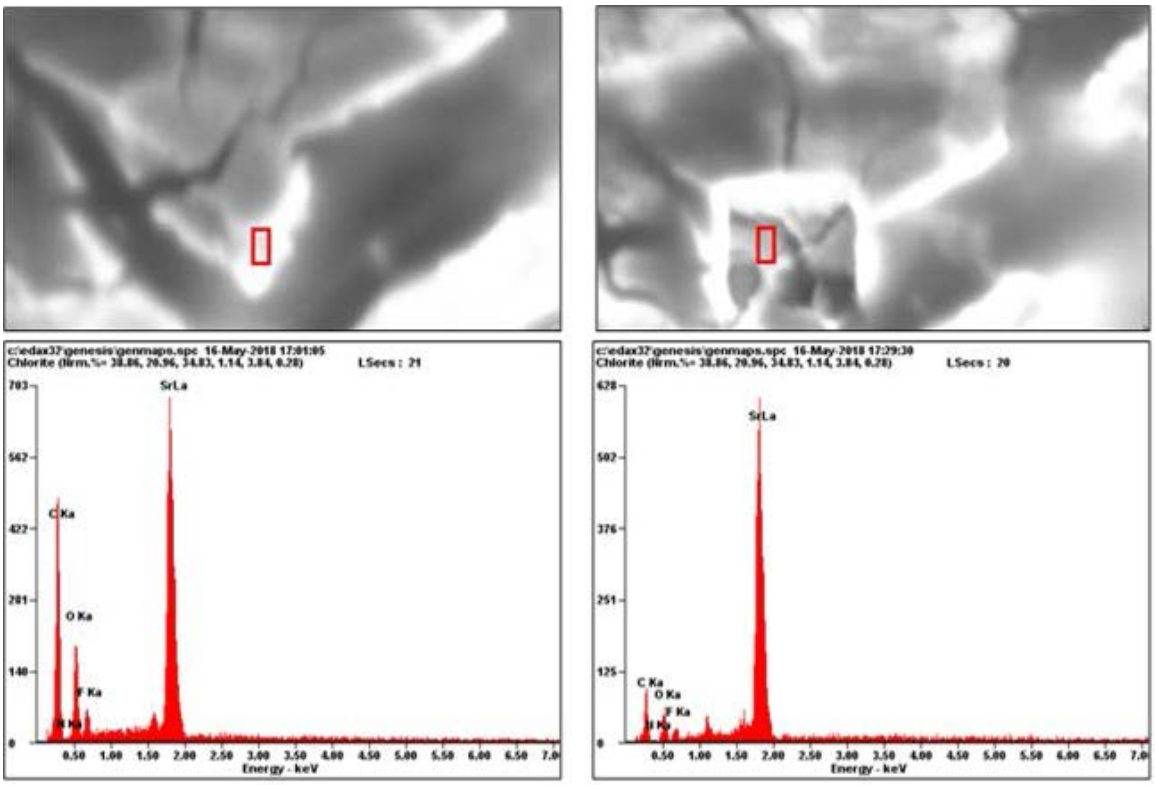

Element	Wt%	At%
CK	53.72	75.96
NK	00.00	00.00
OK	14.45	15.34
FK	03.61	03.23
SrL	28.23	05.47
Matrix	Correction	ZAF

Element	Wt%	At%
CK	33.49	67.49
NK	00.55	00.96
OK	08.52	12.89
FK	02.80	03.57
SrL	54.64	15.10
Matrix	Correction	ZAF

Figure 5.1. Focused ion beam (FIB) images and EDXS data of Sr_2NF taken from different regions of the crystal. Carbon content is likely from the mineral oil used to protect the sample during the crystal selection process. **Left**: Data from the surface shows presence of oxygen; **Right**: data from crystal core, a significant reduction of oxygen is observed.

compared to refinement with no oxygen present (R1(all data) = 0.0246 vs. 0.0242). Given the ordering of anions in the lattice and the magnitude of the unit cell parameter, it is not likely that any oxygen contaminate in the sample is present in large amounts. Based on the above discussion, the present sample was refined as a Sr_2NF phase. The refined model described below would apply whether or not small amounts of oxygen were present.

5.4 Structural Analysis

The refinement had an $Fd\bar{3}m$ (No.227) space group with a doubled cubic crystal system (a=10.6729(3) Å). The unit cell parameter is relatively close to the doubled cubic phase literature value of 10.692(5) Å reported by Wagner (2002). The final R1 (F) value was 0.0242 for all 379 data (18 parameters) and wR2 (F2) was 0.0474. A summary of crystallographic and refinement data is given in **Table 5.1**. Also a further analysis on atomic coordinates, refined occupancy and anisotropic and isotropic displacement parameters is indicated in **Table 5.2**. The Sr atoms are located on one crystallographically distinct site, and are in octahedral coordination to three F atoms and three N atoms. The F and N atoms are each located on distinct crystallographic sites. Doubling of the unit cell relative to the rocksalt-type Sr_2NF is due to the observed ordering of the N and F atoms along the cell edges as displayed in **Figure 5.2**. Excess electron density in the form of the F2 atoms in interstitial tetrahedral sites was refined after the octahedral Sr, N and F positions were selected.

Table 5.1 Refinement data for doubled-cubic Sr_2NF

Identification code	JO_05162016_brown_0m
Empirical formula	Sr_2NF
Formula weight	208.25
Temperature	100(2) K
Wavelength	0.71073 Å
Crystal system	Cubic
Space group	$Fd\bar{3}m$
Unit cell dimensions	a = 10.6729(3) Å
Volume	1215.76(10) $Å^3$
Z	16
Density (calculated)	4.551 Mg/m^3
Absorption coefficient	34.837 mm^{-1}
F(000)	1472.0
Crystal size	0.207 × 0.382 × 0.415 mm^3
Theta range for data collection	3.306 to 52.189°.
Index ranges	0<=h<=16, 0<=k<=16, 1<=l<=23
Reflections collected	598
Independent reflections	379 [R(int) = 0.0376]
Completeness to theta = 25.242°	100.0 %
Absorption correction	Semi empirical from equivalents
Refinement method	Full-matrix least-squares on F^2
Data / restraints / parameters	379/ 2 / 18
Goodness-of-fit on F^2	1.191
Final R indices [I>2sigma(I)]	$R1(F)^a$ = 0.0201, $wR2(F^2)^b$ = 0.0433
R indices (all data)	$R1(F)^a$ = 0.0242, $wR2(F^2)^b$ = 0.0474
Extinction coefficient	0.00000(3)
Largest diff. peak and hole	2.059 and -1.282 $eÅ^{-3}$

[a] $R_1(F) = \Sigma \left| \left| F_o \right| - \left| F_c \right| \right| / \Sigma \left| F_o \right|$ with $F_o > 4.0\sigma(F)$. [b] $wR_2(F^2) = [\Sigma[w(F_o^2 - F_c^2)^2]/\Sigma[w(F_o^2)^2]]^{1/2}$ with $F_o > 4.0\sigma(F)$, and $w^{-1} = \sigma^2(F_o)^2 + (W \cdot P)^2 + T \cdot P$, where $P = (Max(F_o^2,0) + 2F_c^2)/3$, W = 0.0040, and T = 15.3010.

Table 5.2 Atomic coordinates (x 10^4), occupational, and *anisotropic and equivalent isotropic displacement parameters (Å^2 x 10^3) for Sr_2NF.

Atom	$Fd\bar{3}m$ (No. 227) Wyckoff Site	Refined Occ. Factor	No. of Atoms/ Unit Cell	X	Y	Z	U^{11}	U^{23}	U(eq)
Sr1	32e	1.0000	32	81(1)	2419(1)	81(1)	4(1)	0(1)	4(1)
F1	16c	0.7128(2)	11.404(3)	0	5000	0	14(1)	5(1)	14(1)
F1A	32e	0.14835(10)	4.747(3)	305(8)	5305(8)	305(8)	11(2)	-3(2)	11(2)
F2	8b	0.1682(4)	1.346(3)	1250	6250	1250	7(3)	0	7(3)
N1	16d	0.95313(7)	15.250(1)	0	0	0	6(1)	-1(1)	6(1)
F3	16d	0.04684(11)	0.750(2)	0	0	0	6(1)	-1(1)	6(1)

*The anisotropic thermal parameter is expressed as exp [$-2\pi^2(h^2 a^{*2} U_{11} + k^2 b^{*2} U_{22} + l c^{*2} U_{33} + 2hka^*b^*U_{12} + 2 hla^*b^*U_{13} + 2klb^* c^* U_{23})$]; $U_{11} = U_{22} = U_{33}$ and $U_{23} = U_{13} = U_{12}$ for all atoms. U(eq) is defined as one-third of the trace of the Uij orthogonalized tensor. N(1) and F(3) share the 16d site, displacement parameters constrained to be equal.

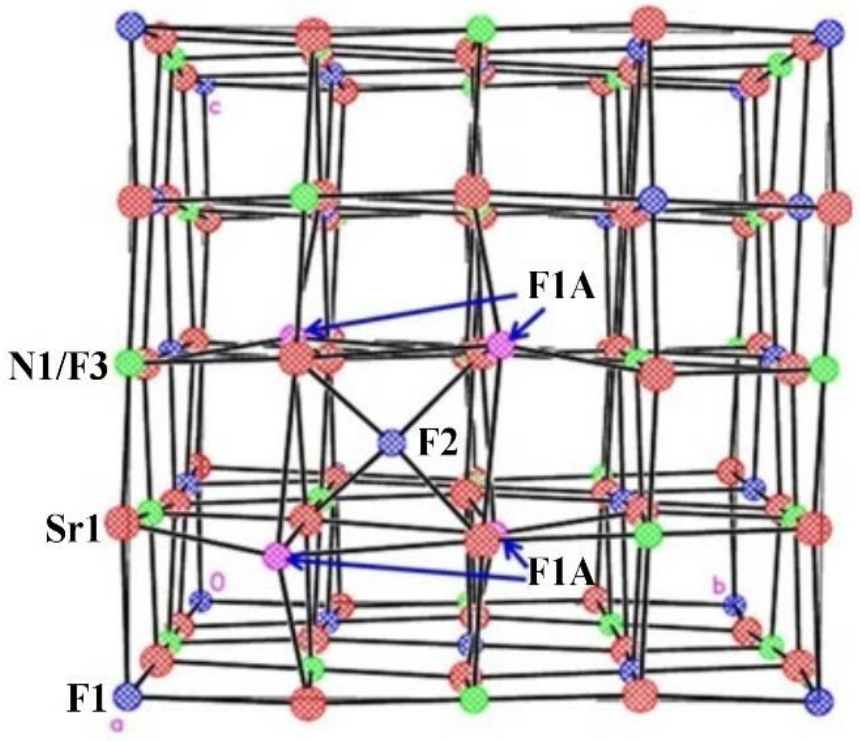

Figure 5.2. Sr_2NF unit cell structure plot showing an interstitial F2 position with adjacent F1A atoms located 0.564(15) Å on opposite sides of F1 atoms (not shown) from which they were likely displaced (see text). Some atoms removed for clarity.

Octahedral sites containing fluorine and nitrogen atoms had observable disorder, but the potential disorder of Sr atoms (displacement by less than 0.1 Å) was rejected. Three distinctive sites associated with the F1 octahedral position that were partially occupied by fluorine atoms were refined. The octahedral F1 position is the F site with the highest occupancy. The disorder at the F1 site is likely a result of the adjacent, partially filled interstitial fluorine (F2) site, and consists of splitting of the F1 position into two symmetrically equivalent positions of F1A displaced by 0.564(15) Å on both sides of F1, pointing to and away from F2 as indicated in **Figure 5.3.** As discussed above, occupancy

of the F1A sites is 4.75 atoms per unit cell, while F2 occupancy is 1.35 atoms per unit cell. This suggests that for each F2 site occupied, approximately four F1A sites are filled. As seen in Figure 5.3, the reason for this shift is due to the short distance of 2.31 Å between F1 and F2, causing the four nearby F1 atoms to shift to the F1A position furthest from the occupied F2 at a more agreeable distance of 2.894 Å away.

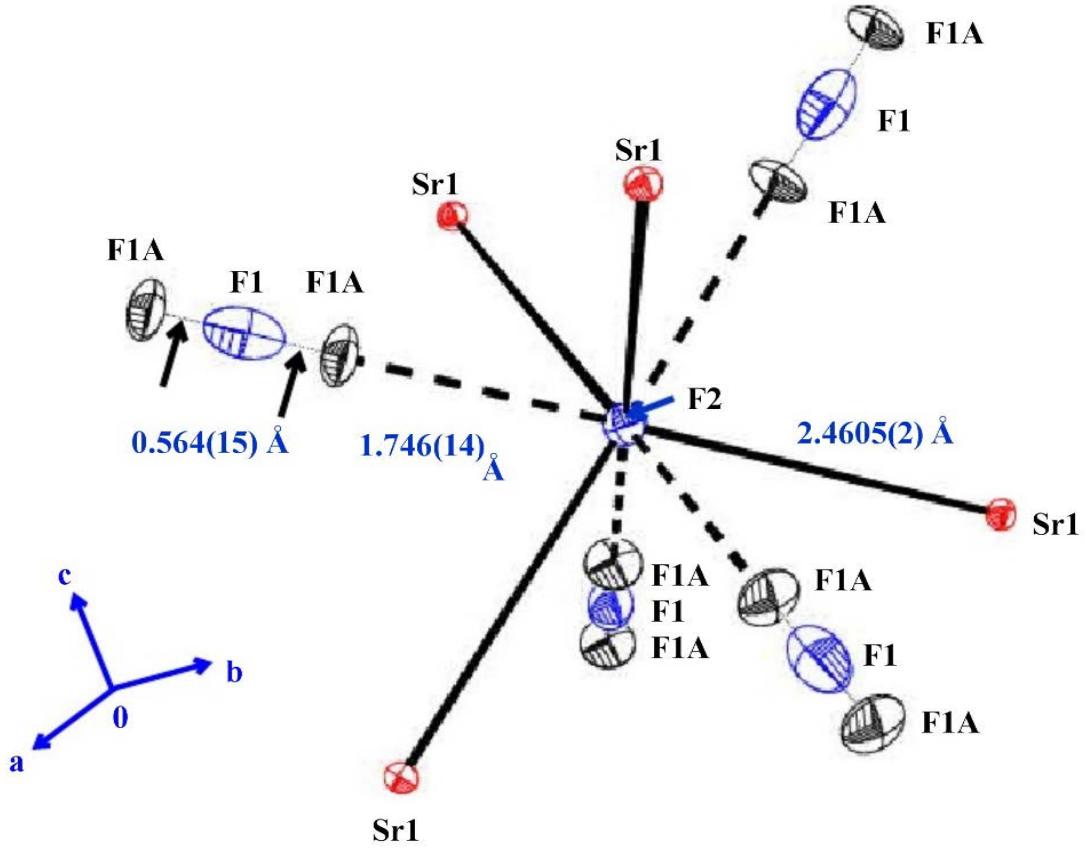

Figure 5.3. F2 environment in Sr_2NF; the F2 atom is the same shown in the unit cell plot in Figure 5.2. F2 is tetrahedrally bonded to Sr. The F1 atom likely moves to the F1A position furthest from the interstitial F2 atom to increase the F2─F1 distance from 2.310 Å to 2.874 Å. 50% ellipsoids.

5.5 Discussion

This work focused on determining whether or not the non-stoichiometric model recently observed for ordered rocksalt-type Ca_2NF (Al-Azzawi *et al*., 2017) using high resolution X-ray diffraction data was present in the Sr_2NF phase as well. As mentioned, previous work within our group on doubled cubic rocksalt-type crystals M_2NF, where M = Ca or Sr, has shown that every refinement revealed the presence of F atoms located at the tetrahedral interstitial sites. The F atom at this interstitial site was previously interpreted to be due to Frenkel defect comprising approximately 10% or higher of F atoms moving to interstitial sites from their octahedral lattice positions. For the more recently proposed non-stoichiometric defect model, excess negative charge due to extra F atoms at the interstitial site are charge balanced by substituting F atoms onto N positions. Specifically, for every two excess F^- ions present, one F^- ion must replace an N^{3-} ion, or alternatively, two O^{2-} ions must replace two N^{3-} ions for charge balance. It follows that the higher the number of excess F atoms present, the lower the N content of the lattice.

Previous work on Sr_2NF reported by Wagner (2002) observed two closely related ordered rocksalt phases with different colors (and presumably compositions), with both refined as Frenkel defects. A brownish yellow (BY) crystal with unit cell parameter a = 10.6920(45) Å and a dark red (DR) crystal with unit cell parameter a = 10.7655(20) Å were reported. As discussed by Al-Azzawi *et al*. (2017), the fact the DR crystal has a larger unit cell parameter as compared to the BY crystal suggests that it has a greater N content in the lattice, and a narrower band gap as all the colors are absorbed other than the red color. The BY crystal has a larger band gap enabling absorption on the violet/blue region, and a lesser amount of N due to the smaller lattice parameter. Thus it

is quite likely that the two phases have different N^{3-}/F^- ratios. This could be due to different excess F content and/or the presence of different amounts of oxygen in the lattice. In terms of the interstitial F content, refinement data indicated that the DR crystal has 1.85 F atom/unit cell, while the BY crystal has 1.68 F atom/unit cell, although these are not present in excess in the Frenkel model.

The Sr_2NF refined here was yellow, and so has a similar color and unit cell parameter as the BY crystal. The present sample has 2.25 excess F atoms per unit cell, with 0.75 F3 atoms per unit cell replacing N atoms, and the remainder at the F2 interstitial site. According to a theoretical study by Fang *et al*. (2003) the band gap decreases as N content increases in going from $MgF_2 – Mg_3NF_3 – Mg_2NF – Mg_3N_2$. The results discussed above for known ordered rocksalt-type Sr_2NF phases appear to be consistent with this trend. This is evident by noting that for these phases, band gaps are expected to decrease going from the colors yellow (Y) to brownish-yellow (BY) to dark red (DR). Also, we expect N content to increase as unit cell parameters increase, or in going from the Y (a = 10.6729(3) Å) to BY (a = 10.6920(45) Å) to DR (a = 10.7655(20) Å) phases discussed above. From this discussion, it is apparent that N content and thus colors of ordered rocksalt M_2NF compounds depend on the amount of excess F atoms in the lattice, as well as whether charge compensation is achieved by substitution of $F^–$ or $O^{2–}$ ions for $N^{3–}$ ions, as this also affects N content.

CHAPTER SIX

SYNTHESIS OF BIMETALLIC NITRIDE FLUORIDES

6.1 Ba-Ca-N-F System

Two samples of BaCaNF were successfully prepared. Each contained a mixture of products, including BaCaNF phases of different Ba:Ca ratios. From the Trial 1 reaction described below, a rocksalt-type sample was analyzed, while Trial 2 yielded a rhombohedral phase. The crystal chemistry of these phases is discussed in Chapter 7.

6.1.1 Trial 1 Synthesis

The synthesis of BaCaNF was thermally treated to a temperature of 900ºC, with Ba, Ca, and BaF_2 having 727ºC, 842ºC and 1368ºC individual melting points, respectively. The rationalization for use of BaF_2 as opposed to CaF_2 in the reaction was that Ba is more reactive than Ca, and therefore Ba^{2+} in BaF_2 should not be reduced by Ca metal. The solid starting materials were stoichiometrically mixed in a glove bag with ratios of two moles of Ca metal to one mole of Ba metal to one mole of BaF_2, all carried out in an argon environment. The three starting materials were weighed on the balance scale, with 2.0g of Ba metal, 1.4g of Ca metal, and 3.2g BaF_2 in the reaction mixture. A nickel crucible was utilized to load in the starting materials which were transferred into the Inconel tube for high temperature reaction. The overall chemical reaction is summarized below:

$$BaF_2 + Ba + 2Ca + N_2 \rightarrow 2BaCaNF$$

Within the Inconel furnace tube, the mixture of the stoichiometric starting materials was heated initially with argon gas flow then cooled and switched to nitrogen

gas flow before reheating. The following furnace program was used for the reaction cycle (R = Ramp function, L = Temperature level, and D = Dwell time):

Step 1: R1 Step Function L1 100ºC D1 0 Hours

Step 2: R2 60ºC /hr. L2 900ºC D2 1 Hours

Step 3: R3 100ºC /hr. L3 200ºC D3 4 Hours

Step 4: R4 60ºC /hr. L4 900ºC D4 4 Hours

Step 5: R5 15ºC /hr. L5 200ºC D5 0 Hours

Step 6: R6 Step Function L6 70ºC D6 End

Argon gas is switched to nitrogen gas on the third dwell. The product was removed from the Inconel tube and transferred to the glove bag under the argon gas flow. It consisted of a mixture of violet and red crystals within a black chunk. A sample of the product was placed in a glass slide containing mineral oil for analysis on the optical microscope. This process is vital in protecting the sample from air while expediting the selection of a good single crystal for X-Ray data collection.

6.1.2 Trial 2 Synthesis

For this trial, the reaction mixture was heated to a temperature of 1000ºC. Here, CaF_2 (melting point 1418 ºC) was used as a reactant instead of BaF_2 as in Trial 1. This was to determine what, if any, impact the change would have on reaction outcome. Not much change was expected (or observed), as any reduced Ca^{2+} would likely re-oxidize under N_2 gas. The solid starting materials were weighed on the balance and mixed in the following proportions: 2.5g (0.018 moles) of Ba metal, 0.7g (0.009 moles) of CaF_2 and

0.4g (0.009 moles) of Ca metal. These were placed inside a nickel crucible covered with a lid slightly open, which was placed inside a nickel boat and then transferred to the Inconel tube in the Themolyne furnace. The overall chemical reaction is summarized below:

$$CaF_2 + 2Ba + Ca + N_2 \rightarrow 2BaCaNF$$

The furnace program utilized for the reaction cycle is given below (R = Ramp function, L = Temperature level, and D = Dwell time):

Step 1: R1 Step Function L1 100ºC D1 0 Hours

Step 2: R2 60ºC /hr. L2 1000ºC D2 1 Hours

Step 3: R3 100ºC /hr. L3 200ºC D3 4 Hours

Step 4: R4 60ºC /hr. L4 1000ºC D4 4 Hours

Step 5: R5 12ºC /hr. L5 200ºC D5 0 Hours

Step 6: R6 Step Function L6 70ºC D6 End

The argon gas flow was switched to nitrogen after the third dwell and starting with the fourth step of the furnace program. The product mixture, which consisted of black chunks with red crystallites and other grey shining crystals, was removed from the Inconel tube onto a glass slide containing mineral oil, and taken to the X-ray lab for crystal selection and X-ray data collection.

6.2 Ba-Sr-N-F System

Two samples of BaSrNF were successfully prepared. Each contained a mixture of products, including BaSrNF phases of different Ba:Sr ratios. From the Trial 1

preparation, a rocksalt-type sample was analyzed, while Trial 2 yielded a doubled cubic phase. The crystal chemistry of these phases is discussed in **Chapter 7**.

For both trials, compounds in the Ba-Sr-N-F system were prepared by the reaction:

$$SrF_2 + 2Ba + Sr + N_2 \rightarrow 2BaSrNF$$

These reactants were heated to a target temperature of 1000ºC with Ba, Sr and SrF_2 having melting points of 727ºC, 769 ºC and 1477ºC respectively. The solid stoichiometric starting materials were placed inside a glove bag under argon where mixing was done to prevent any contamination, since the metal reactants are air sensitive and could react easily in air.

6.2.1 Trial 1 Synthesis

The reactants were weighed on the balance and the masses of 2.5g (0.018 moles) of Ba metal, 1.1g (0.009 moles) of Sr metal, and 1.1g (0.009 moles) of SrF_2 were placed in a nickel crucible, which was in turn placed an a nickel boat and then transferred to the Inconel tube within the Thermolyne furnace.

The reaction employed the following furnace program (R = Ramp Rate, L = Temperature Level, and D = Dwell Time):

Step 1: R1 Step Function L1 100ºC D1 0 Hours

Step 2: R2 60ºC /hr. L2 1000ºC D2 1 Hours

Step 3: R3 100ºC /hr. L3 200ºC D3 4 Hours

Step 4: R4 60ºC /hr. L4 1000ºC D4 4 Hours

Step 5: R5 12ºC /hr. L5 200ºC D5 0 Hours

Step 6: R6 Step Function L6 70ºC D6 End

The switch from argon to nitrogen gas occurred during the third step, at the 4 hr dwell at 200ºC, where it was maintained (nitrogen gas flow) until the last step. The product mixture was composed of red and violet crystals embedded in black chunks of powdered material.

6.2.2 Trial 2 Synthesis

Masses of 2.5g (0.018 moles) of Ba metal, 1.1g (0.009 moles) Sr metal, and 1.1g (0.009 moles) of SrF_2 were placed in a nickel crucible, which was then placed on a nickel boat and transferred to the Inconel tube within the Thermolyne furnace. The reaction employed the following furnace program (R = Ramp Rate, L = Temperature Level, and D = Dwell Time), which differed from the Trial 1 program only by the number of hours that the melt was held at high temperature before slow cooling:

Step 1: R1 Step Function L1 100ºC D1 0 Hours

Step 2: R2 60ºC /hr. L2 1000ºC D2 1 Hours

Step 3: R3 100ºC /hr. L3 200ºC D3 4 Hours

Step 4: R4 60ºC /hr. L4 1000ºC D4 6 Hours

Step 5: R5 15ºC /hr. L5 200ºC D5 0 Hours

Step 6: R6 Step Function L6 70ºC D6 End

The switch from argon to nitrogen gas again occurred during the third step. The product mixture was again composed of red and violet crystals embedded in chunks of black powder.

6.3 Attempted Synthesis of BaMgNF

In the interest of focusing on the BaMNF systems with M = another Group II metal besides Ba, attempts were also made to synthesize Ba-Mg-N-F compounds.

The synthesis attempts were carried out by the following chemical equation:

$$MgF_2 + 2Ba + Mg + N_2 \rightarrow 2BaMgNF$$

The starting materials MgF_2, Ba, and Mg have melting points of 1263 °C, 727°C and 650°C, respectively. The target reaction temperature was at 1000ºC to ensure that the reactants formed a melt for the single crystal growth. The reactants in the glove bag under argon gas flow had the following masses on the balance 2.5g (0.018 moles), 0.7g (0.009 moles) and 0.2g (0.009 moles) for Ba, MgF_2 and Mg, respectively. The mixtures were placed in a nickel crucible and into a nickel boat and then transferred to the Inconel reaction tube in the furnace. The following is the furnace program that was used in running the reaction (R = Ramp function, L = Temperature level, D = Dwell function):

Step 1:	R1	Step Function	L1	70ºC	D1 0 Hours
Step 2:	R2	80ºC /hr.	L2	1000ºC	D2 4 Hours
Step 3:	R3	80ºC /hr.	L3	200ºC	D3 2 Hours
Step 4:	R4	60ºC /hr.	L4	1000ºC	D4 4 Hours
Step 5:	R5	15ºC /hr.	L5	200ºC	D5 0 Hours

Step 6: R6 Step Function L6 70ºC D6 0 Hours

Step 7: End

Synthesis attempts (two attempts) yielded black powdery chunks containing red crystals. The samples analyzed (as indicated by their unit cell parameters) were all known binary phases Ba-N-F and Mg-N-F compounds. No mixed metal phases were observed. It is possible that the binary phases are more stable than rocksalt-type mixed metal BaMgNF phases due to the large difference in sizes of Ba vs Mg atoms. For example, the Ba/Mg size ratio is 2.37, whereas Ba/Ca is 1.35 and Ba/Sr is 1.14. It was expected that a quadrupled phase might be found, but this has not been the case so far. Such a phases was prepared in the Ca-Mg-N-F system by Al-Azzawi (2016), with Ca/Mg size ratio of 1.75.

CHAPTER SEVEN

RESULTS AND DISCUSSION OF BIMETALLIC NITRIDE FLUORIDES

7.1 BaCaNF system – Trial 1 Sample, Disordered Rocksalt

The Trial 1 synthesis for BaCaNF was outlined in **Section 6.1.1**. With the reaction complete, a small amount of the sample product was selected in an argon filled glove bag and placed in mineral oil on a glass slide. The sample had black powdery chunks, red crystallites, and grey shiny crystallites in the product mixture. One of the multi-crystalline samples was selected and broken further to isolate a single crystal. The red crystal selected was mounted on the Bruker D8 Quest single crystal diffractometer described in **Section.4.1.** The unit cell was determined from 283 reflections using the program *Cell Now* called from Bruker's APEX3 program. Of these, 246 reflections were exclusively indexed to the cubic unit cell (see below), the remaining 37 were not assigned to a domain. A full-sphere of intensity data was collected to a resolution of 0.49 Å.

The space group found for BaCaNF crystal was $Fm\bar{3}m$ suggesting that it was a rocksalt-type with Z= 2; a = 5.5361(44) Å. This unit cell parameter lies at just over ¾ of the gap spanning the difference between the parameters for Ca_2NF, a = 4.9861(11) Å (Strozewski, 2007) and Ba_2NF, a = 5.6796(19) Å (Seibel & Wagner, 2004). Assuming that the cell parameter for Ca_2NF increases in a roughly linear fashion as Ca is replaced by Ba to ultimately yield Ba_2NF suggests that this BaCaNF crystal should have a Ba:Ca ratio of 0.79:0.21, or a composition of $Ba_{1.58}Ca_{0.42}NF$. The actual refined composition was $Ba_{1.66}Ca_{0.34}NF$. A unit cell plot is shown in **Figure 7.1**., where it is seen that the Ba^{2+} and Ca^{2+} metal ions share a site, as do the N^{3-} and F^{-} anions. The data was refined to a 0.49 Å resolution. Additional refinement and crystallographic data are summarized

in **Table 7.1**. Atomic coordinates, occupational and anisotropic and equivalent isotropic displacement parameters maybe found in **Table 7.2**.

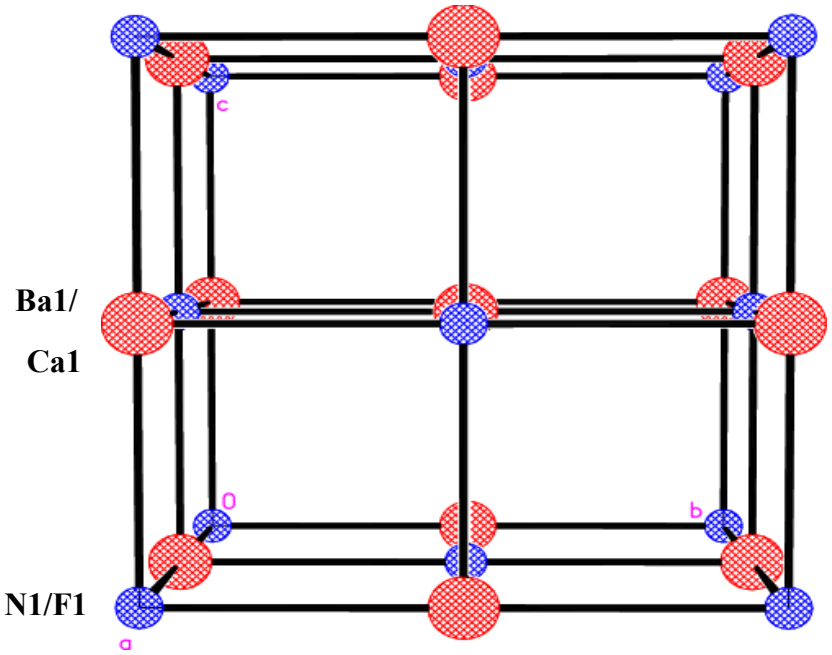

Figure 7.1. Unit cell plot from single crystal X-ray diffraction for rocksalt-type BaCaNF system, a = 5.5361(44) Å, showing Ba/Ca and N/F each sharing a site.

The structure refinement was very straightforward, with the model yielding low R values of R1(F) = 0.0096 and wR2(F^2) = 0.0233 for all 59 unique reflections (5 parameters). Both cation and anion sites are disordered, with random distribution of Ba^{2+} & Sr^{2+} and N^{3-} & F^- ions sharing their respective positions. No further disorder (e.g. displacement of ions at either site, etc.) was observed. The Ba/Ca – N/F bond length is 2.7681(8) Å.

Table 7.1 Crystal data and structure refinement for rocksalt-type BaCaNF

Identification code	17JOBaCaNF_2a_0m
Empirical formula	BaCaNF
Formula weight	210.43
Temperature	100(2) K
Wavelength	0.71073 Å
Crystal system	Cubic
Space group	$Fm\bar{3}m$
Unit cell dimensions	a = 5.5361(15) Å
Volume	169.67(14) $Å^3$
Z	2
Density (calculated)	4.119 Mg/m^3
Absorption coefficient	12.979 mm^{-1}
F(000)	184.0
Crystal size	0.0200 × 0.0217 × 0.0400 mm^3
Theta range for data collection	6.383 to 46.571°.
Index ranges	-11<=h<=5, -8<=k<=11, -9<=l<=10
Reflections collected	556
Independent reflections	59 [R(int) = 0.0250]
Completeness to theta = 25.242°	100.0 %
Absorption correction	Multi-scan
Refinement method	Full-matrix least-squares on F^2
Data / restraints / parameters	59 / 1 / 5
Goodness-of-fit on F^2	1.015
Final R indices [I>2sigma(I)]	$R1(F)^a$ = 0.0096, $wR2(F^2)^b$ = 0.0233
R indices (all data)	$R1(F)^a$ = 0.0096, $wR2(F^2)^b$ = 0.0233
Extinction coefficient	0.00022(7)
Largest diff. peak and hole	1.172 and -1.209 $eÅ^{-3}$

[a] $R_1(F) = \Sigma \left| \left| F_o \right| - \left| F_c \right| \right| / \Sigma \left| F_o \right|$ with $F_o > 4.0\sigma(F)$. [b] $wR_2(F^2) = [\Sigma[w(F_o^2 - F_c^2)^2]/\Sigma[w(F_o^2)^2]]^{1/2}$ with $F_o > 4.0\sigma(F)$, and $w^{-1} = \sigma^2(F_o)^2 + (W \cdot P)^2 + T \cdot P$, where $P = (Max(F_o^2,0) + 2F_c^2)/3$, W = 0.0196, and T = 0.00.

Table 7.2. Atomic coordinates (x 10^4), occupational, and *anisotropic, and equivalent isotropic displacement parameters ($Å^2$x 10^3) for disordered rocksalt-type BaCaNF.

Atom	Wyckoff Site	Refined Occ. Factor	X	Y	Z	U^{11}	U^{23}	U(eq)
Ba1	4b	0.41052	0	5000	5000	6(1)	0	6(1)
Ca1	4b	0.58948	0	5000	5000	6(1)	0	6(1)
F1	4a	0.500	0	5000	0	12(1)	0	12(1)
N1	4a	0.500	0	5000	0	12(1)	0	12(1)

*The anisotropic thermal parameter is expressed as exp [$-2\pi^2(h^2 a^{*2} U_{11} + k^2 b^{*2} U_{22} + l c^{*2} U_{33} + 2hka^*b^*U_{12} + 2 hla^*b^*U_{13} + 2klb^* c^* U_{23})$]; $U_{11} = U_{22} = U_{33}$ and $U_{23} = U_{13} = U_{12}$ for all atoms. U(eq) is defined as one-third of the trace of the Uij orthogonalized tensor. Ba1 & Ca1 and F1 & N1 share their respective sites, with respective displacement parameters constrained to be equal.

7.2 BaCaNF system – Trial 2 Sample, Rhombohedral

The space group found for the Trial 2 BaCaNF crystal was $R\bar{3}m$ indicating a rhombohedral cell type, which had Z = 3. The unit cell was determined from 315 reflections using the program *Cell Now* called from Bruker's APEX3 program. Of these, 314 reflections were exclusively indexed to the rhombohedral unit cell (see below), the remaining 1 reflection was not assigned to a domain.

The unit cell parameters (hexagonal axes) for this BaCaNF sample were a = b = 3.9646(3) Å; c = 19.7792(17); Vol. = 269.245(63) $Å^3$. These are close to the literature values for Ba_2NF: a = b = 4.0242(2) Å; c = 19.975(1), and Vol. = 280.14 $Å^3$, as reported by Bailey *et al*. (2011). The final R1 value at convergence was 0.0232 (all data), and the structure was refined to 0.54 Å resolution. The refined composition is $Ba_{1.82}Ca_{0.18}NF$, and

the substitution of the small quantity of Ca^{2+} for larger Ba^{2+} ions is consistent with the decreased cell volume observed for the new phase relative to the Ba_2NF rhombohedral lattice. This is the first bimetallic nitride fluoride compound to crystallize in the rhombohedral crystal system. Refinement data is given in **Table 7.3**, and atomic coordinates, occupational and anisotropic and equivalent isotropic displacement parameters maybe found in **Table 7.4**.

The structure plot is given in **Figure 7.2**, and shows $[Ba_2N]^+$ layers separated by F^- ions positioned at octahedral sites. The Ba_2NF phase reported by Bailey *et al*. (2011) and now the BaCaNF phase presented here are the only nitride fluorides known to crystallize with this layered rhombohedral lattice. Other M_2NF compounds for M = Mg, Ca, or Sr typically crystallize in the disordered or ordered rocksalt-type phases, or the tetragonal L-Mg_2NF-type phase discussed in Chapter 1. Due to repulsions between the $[M_2N]^+$ layers in the rhombohedral phase, this structure is favored by M_2NX compounds where X = a large halide ion such as Cl^- or Br^- that increase the $[M_2N]^+$ interlayer distance (d in Figure 7.2), and therefore minimize interlayer repulsions. The large Ba^{2+} ion in $[Ba_2N]^+$ layers, forming long bonds to F^- ions, also increases the interlayer distance (d) enough to minimize repulsions. If d is too small, perhaps less than around 3.5 Å (see Bailey *et al*., 2011), the interlayer repulsions are then too large and the ordered (or disordered) rocksalt-type structures are preferred. For hypothetical Ca_2NF and Sr_2NF layered-rhombohedral phases, d is estimated (Bailey et al., 2011) to be only 2.88 Å and 3.03 Å, respectively. Thus, these phases have never been observed. Instead, they crystallize as rocksalt or doubled cubic phases which are not layered and so have no interlayer repulsions. Interestingly, the interlayer distance for the $Ba_{1.82}Ca_{0.18}NF$ phase

presented here is 3.573 Å, larger than the value for Ba_2NF of 3.518 Å reported by Bailey et al. (2011). This may be due to distortions in the $N(Ba_{5.46}Ca_{0.54})$ vs. NBa_6 octahedra.

Table 7.3. Refinement data for rhombohedral BaCaNF

Identification code	17JOBaCaNF_3a_0m
Empirical formula	BaCaNF
Formula weight	210.43
Temperature	100(2) K
Wavelength	0.71073 Å
Crystal system	Rhombohedral
Space group	$R\bar{3}m$
Unit cell dimensions	a = 3.9646(3) Å
Volume	269.24(10) $Å^3$
Z	3
Density (calculated)	3.894 Mg/m^3
Absorption coefficient	12.269 mm^{-1}
F(000)	276
Crystal size	0.174 × 0.247 × 0.296 mm^3
Theta range for data collection	3.090 to 41.289°.
Index ranges	-6<=h<=0, -0<=k<=7, -0<=l<=36
Reflections collected	270
Independent reflections	270 [R(int) = 0.0705]
Completeness to theta = 25.242°	100.0 %
Absorption correction	Multi-scan
Refinement method	Full-matrix least-squares on F^2
Data / restraints / parameters	270 / 0 / 11
Goodness-of-fit on F^2	1.197
Final R indices [I>2sigma(I)]	$R1(F)^a$ = 0.0185, $wR2(F^2)^b$ = 0.0399
R indices (all data)	$R1(F)^a$ = 0.0237, $wR2(F^2)^b$ = 0.0413
Extinction coefficient	0.00010(18)

[a] $R_1(F) = \Sigma \left| \left| F_o \right| - \left| F_c \right| \right| / \Sigma \left| F_o \right|$ with $F_o > 4.0\sigma(F)$. [b] $wR_2(F^2) = [\Sigma[w(F_o^2 - F_c^2)^2]/\Sigma[w(F_o^2)^2]]^{1/2}$ with $F_o > 4.0\sigma(F)$, and $w^{-1} = \sigma^2(F_o)^2 + (W \cdot P)^2 + T \cdot P$, where $P = (Max(F_o^2,0) + 2F_c^2)/3$, W = 0.0195 , and T = 2.0788.

Table 7.4. Atomic coordinates (x 10^4), occupational, and anisotropic, and equivalent isotropic displacement parameters (Å^{2}x 10^3) for rhombohedral BaCaNF.

Atom	Wyckoff Site	Refined Occ. Factor	X	Y	Z	U^{11}	U^{33}	U^{23}	U^{12}	U(eq)
Ba1	6c	0.911	3333	6667	4097(1)	6(1)	7(1)	0	3(1)	6(1)
Ca1	6c	0.089	3333	6667	3885(6)	6(1)	7(1)	0	3(1)	6(1)
F1	3b	1.000	0	10000	5000	23(2)	22(2)	0	11(2)	22(1)
N1	3a	1.000	6667	3333	3333	9(1)	15(2)	0	4(1)	11(1)

*The anisotropic thermal parameter is expressed as exp $[-2\pi^2(h^2 a^{*2} U_{11} + k^2 b^{*2} U_{22} + l c^{*2} U_{33} + 2hka^*b^*U_{12} + 2 hla^*b^*U_{13} + 2klb^* c^* U_{23})]$; $U_{11} = U_{22}$ and $U_{23} = U_{13}$ for all atoms. U(eq) is defined as one-third of the trace of the Uij orthogonalized tensor. Ba(1) and Ca(1) share the 6c site, although they are displaced 0.419 Å apart; displacement parameters constrained to be equal.

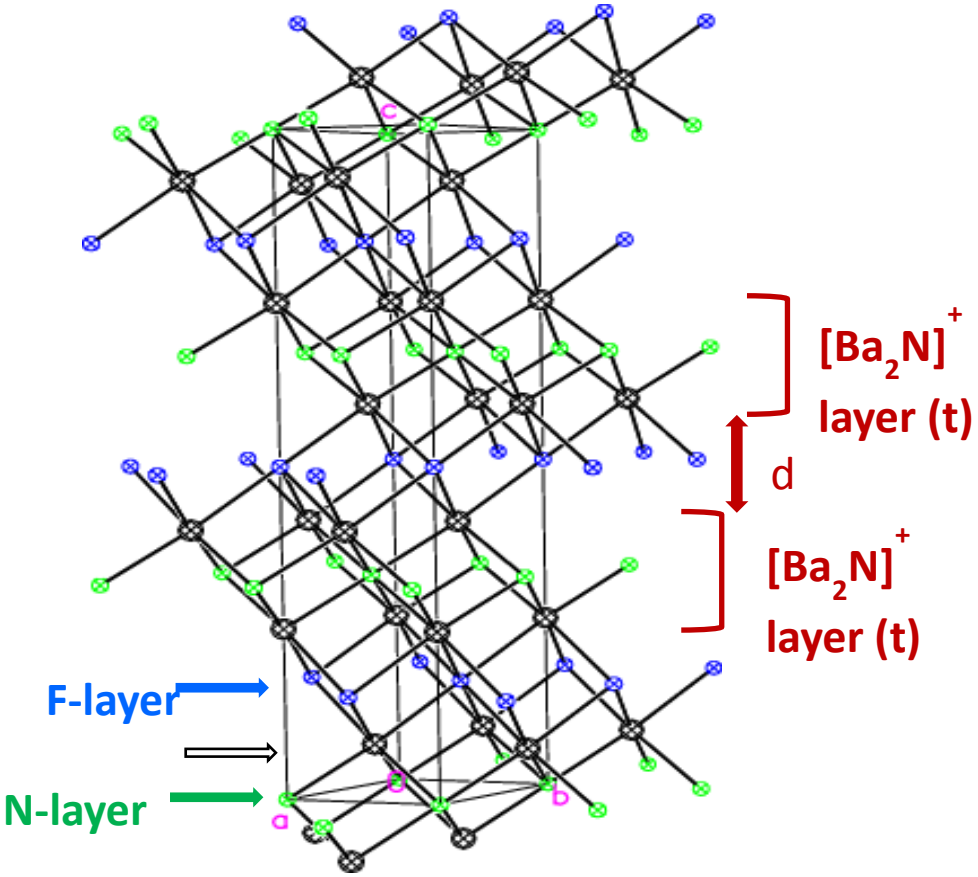

Figure 7.2. A view of the unit cell for the final structure of layered-rhombohedral BaCaNF. The structure consists of $[Ba_2N]^+$ layers separated by a layer of F^- ions. The distance (d) between layers regulates the level of $[Ba_2N]^+$ repulsion occurring in the lattice.

Figure 7.3 shows the local coordination environment of the Ba/Ca site, where it is seen that Ca is somewhat displaced from the Ba position by about 0.419 Å. The refinement of Ba and Ca atoms to separate positions resulted in reduction of R1/wR2 values from 0.0364/0.1083 to 0.0224/0.0771. This is because Ca atoms located at the Ba position are significantly underbonded, and so move closer to N atoms in order to increase bonding interactions. This can be shown by use of the bond valence calculation method and empirical parameters presented by Brese and O'Keeffe (1991). The method utilizes the equation $V_{ij} = \exp[R_{ij}-d_{ij})/0.37]$ to calculate a bond valence, v_{ij}, for each i-j pair of atoms bonded together at bond length d_{ij}. The sum of v_{ij} around a specific central atom in a coordination sphere in the lattice gives V_{ij}, which ideally equals the valence of the central atom (e.g., +2 for Ba). R_{ij} is an empirical parameter derived from high quality X-ray diffraction data from crystals containing the bond i-j of interest. **Table 7.5** shows selected bonds lengths and bond angles, while **Table 7.6** shows the results of the bond valence analysis for this rhombohedral BaCaNF phase. It is seen from Table 7.6 that when Ca moves from the Ba site to a position closer to the N^{3-} ions, its bond valence sum increases, thus explaining the observed displacement of the Ca atom from the Ba site by 0.419 Å. The significant underbonding of Ca of 1.11 valence units (relative to its ideal valence of 2) at its displaced site is due to its low occupancy relative to Ba. The higher occupancy of Ba expands the coordination sphere, elongating Ca-N/F bonds.

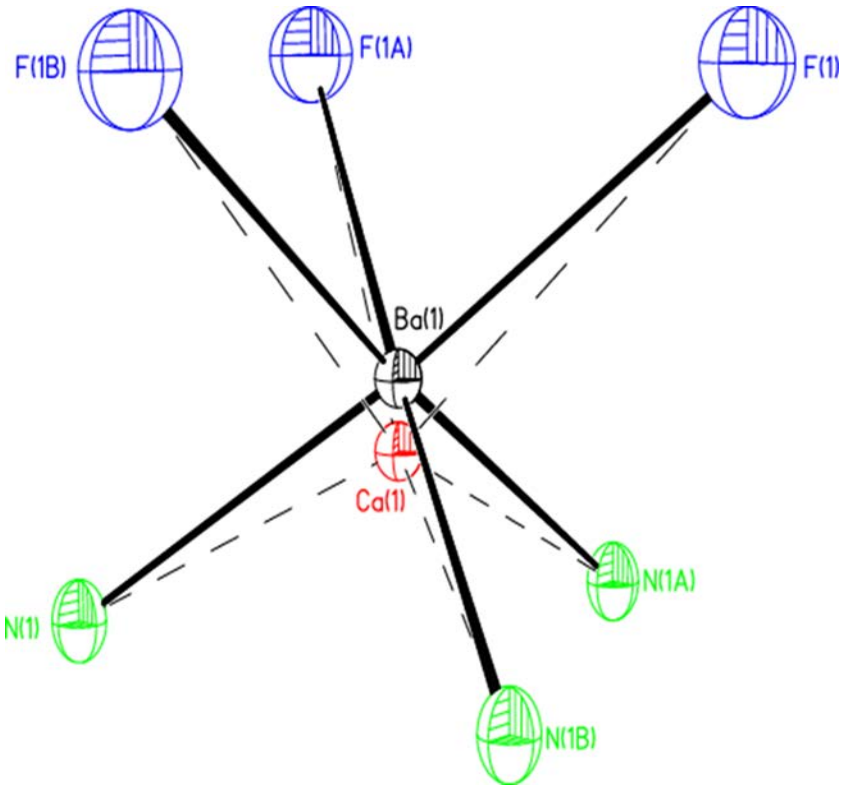

Figure 7.3. A view of Ba/Ca coordination sphere in the rocksalt BaCaNF structure. Ba/Ca share a site but Ca is underbonded, the distance between Ba-Ca is 0.419 Å.

Table 7.5. Selected bond lengths (Å) and angles (°) for rhombohedral BaCaNF

Bond lengths (Å)			
Ca(1)−N(1):	2.536(2)	Ca(1)−F(1):	3.178
Ba(1)− N(1):	2.7423(2)	Ba(1)−F(1):	2.9035(3)

Bonded or non-bonded angles (°)	
N1/F3−Ba−N1/F3	92.583(9)
N1−Ba−F1	175.418(11)
F(1)−Ba(1)−F(1)	86.116(9)
F(1)−Ba(1)−Ca(1)	136.24(2)
N(1)−Ba(1)−Ca(1)	92.92(15)

Table 7.6. Bond Valence calculations for rhombohedral BaCaNF

Anions	***Bond Valences, v_{ij} $v_{ij} = \exp[(R_{ij} - d_{ij})/0.37)$**		
	Ba(1)	**Ca(1)**	**Ca(1) at Ba(1) Site**
N(1)	0.479 × 3	0.343 × 3	0.196 × 3
F(1)	0.145 × 3	0.0270 × 3	0.0568 × 3
Sum for Cations, $V_{ij} = \Sigma v_{ij}$	**1.872**	**1.11**	**0.758**

7.3 BaSrNF System – Trial 1 Sample, Disordered Rocksalt

An orange crystal was analyzed using the Bruker D8 Quest single crystal X-Ray diffractometer (see Section 4.1) and the final phase was a Sr-rich one. The space group found for the BaSrNF crystal was $Fm\bar{3}m$, suggesting that it was a rocksalt type with Z= 2 and a = 5.4783(2) Å. The unit cell was determined from 686 reflections using the program *Cell Now* called from Bruker's APEX3 program. Of these, 513 reflections were exclusively indexed to the cubic unit cell (see below), the remaining 173 were not assigned to a domain, thus the sample was multi-crystalline. These crystallites were not related by twin laws. A full-sphere of intensity data was collected to a resolution of 0.49 Å. Refinement data is summarized in **Table 7.7**, and atomic coordinates, occupational and anisotropic and equivalent isotropic displacement parameters maybe found in **Table 7.8**.

The unit cell of a = 5.4783(2) Å for this phase lies at about 46% of the gap between the disordered rocksalt end members from Sr_2NF (a = 5.3051(2) Å; Keino, 2017) to Ba_2NF (a = 5.6796(19) Å; Seibel & Wagner, 2004), suggesting a relatively rich Sr-phase. Accordingly, the refined composition is $Ba_{0.82}Sr_{1.18}NF$, or 41% Ba, 59% Sr. The unit cell structure plot is shown in **Figure 7.4**, and the local Ba/Sr coordination environment is shown in **Figure 7.5**, with 75% ellipsoids. These figures indicate a well-behaved structure. The Ba/Sr metals share a site and similarly the N/F anions share a site, with neither site showing atom displacement. The final R1/wR2 values were 0.0164/0.0365 (all 51 data), and the structure was refined to 0.53 Å resolution. The Ba/Sr – N/F bond length is 2.73915(10) Å.

Table 7.7 Refinement data for rocksalt-type BaSrNF

Identification code	17JOBaSrNF_2a_0m
Empirical formula	BaSrNF
Formula weight	257.97
Temperature	100(2) K
Wavelength	0.71073 Å
Crystal system	Cubic
Space group	$Fm\bar{3}m$
Unit cell dimensions	a = 5.4783(2) Å
Volume	164.413(10) $Å^3$
Z	2
Density (calculated)	5.211 Mg/m^3
Absorption coefficient	27.882 mm^{-1}
F(000)	220.0
Crystal size	0.0663 × 0.0553 × 0.0190 mm^3
Theta range for data collection	6.45 to 42.39°.
Index ranges	-10<=h<=10, -10<=k<=10, -10<=l<=10
Reflections collected	6238
Independent reflections	51 [R(int) = 0.0705]
Completeness to theta = 25.242°	100.0 %
Absorption correction	Multi-scan
Refinement method	Full-matrix least-squares on F^2
Data / restraints / parameters	51 / 1 / 6
Goodness-of-fit on F^2	1.329
Final R indices [I>2sigma(I)]	$R1(F)^a$ = 0.0159, $wR2(F^2)^b$ = 0.0365
R indices (all data)	$R1(F)^a$ = 0.0164, $wR2(F^2)^b$ = 0.0365
Extinction coefficient	0.00010(18)
Largest diff. peak and hole	0.69 and -1.19 $eÅ^{-3}$

[a] $R_1(F) = \Sigma \left| \left| F_o \right| - \left| F_c \right| \right| / \Sigma \left| F_o \right|$ with $F_o > 4.0\sigma(F)$. [b] $wR_2(F^2) = [\Sigma[w(F_o^2 - F_c^2)^2]/\Sigma[w(F_o^2)^2]]^{1/2}$ with $F_o > 4.0\sigma(F)$, and $w^{-1} = \sigma^2(F_o)^2 + (W \cdot P)^2 + T \cdot P$, where $P = (Max(F_o^2,0) + 2F_c^2)/3$, W = 0.0187 , and T = 0.5818.

Table 7.8. Atomic coordinates (x 10^4), occupational, and *anisotropic, and equivalent isotropic displacement parameters (Å^{2}x 10^3) for rocksalt-type BaSrNF.

Atom	Wyckoff Site	Refined Occ. Factor	X	Y	Z	U^{11}	U^{23}	U(eq)
Ba1	4b	0.41052	5000	5000	5000	15(1)	0	15(1)
Sr1	4b	0.58948	5000	5000	5000	15(1)	0	15(1)
F1	4a	0.500	0	5000	5000	26(2)	0	26(1)
N1	4a	0.500	0	5000	5000	26(1)	0	26(1)

*The anisotropic thermal parameter is expressed as exp [$-2\pi^2(h^2 a^{*2} U_{11} + k^2 b^{*2} U_{22} + l c^{*2} U_{33} + 2hka^*b^*U_{12} + 2 hla^*b^*U_{13} + 2klb^* c^* U_{23})$]; $U_{11} = U_{22} = U_{33}$ and $U_{23} = U_{13} = U_{12}$ for all atoms. U(eq) is defined as one-third of the trace of the Uij orthogonalized tensor. Ba1 & Sr1 and F1 & N1 share their respective sites, with respective displacement parameters constrained to be equal.

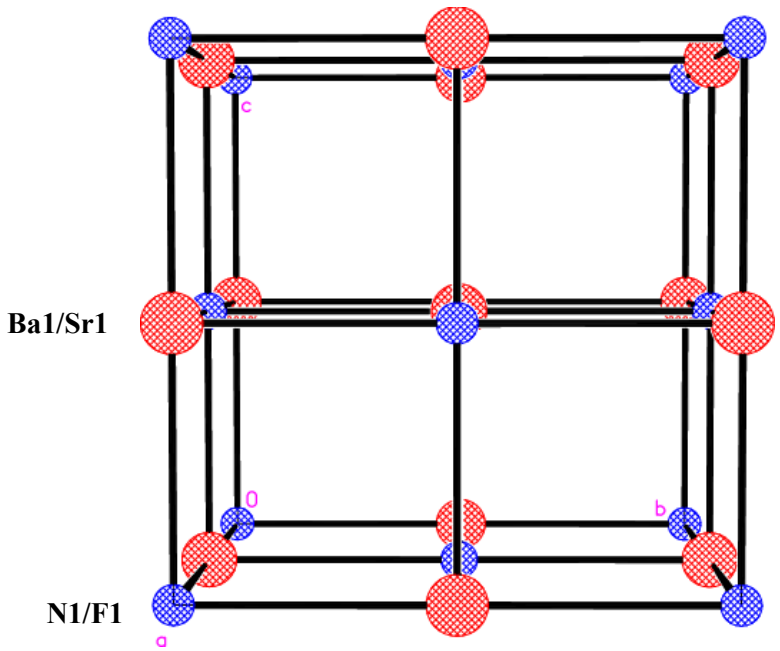

Figure 7.4. A structure plot from single crystal X-ray diffraction for rocksalt BaSrNF system showing sharing of respective sites for Ba/Sr and N/F.

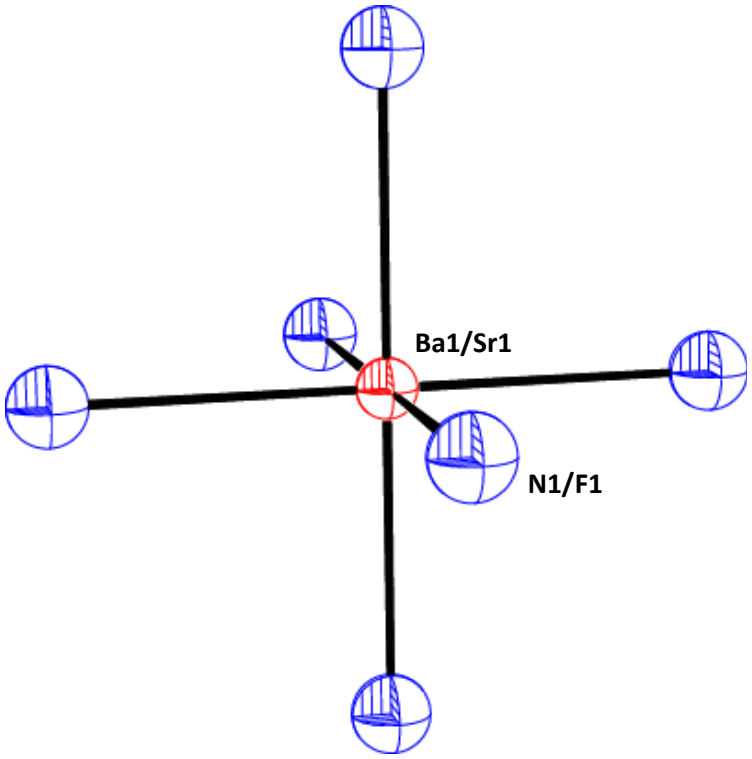

Figure 7.5. Ba/Sr environment of rocksalt-type BaSrNF; 75% ellipsoids.

7.4 BaSrNF System – Trial 2 Sample, Ordered Rocksalt

A brown crystal was selected for analysis using the Bruker D8 single crystal X-ray diffractometer (see Section 4.1) and the final phase was found to be Sr-rich. The cubic unit cell of a = 10.8637(9) Å was determined from 1246 reflections using the program *Cell Now* called from Bruker's APEX3 program. Of these, 1232 reflections were exclusively indexed to the cubic unit cell, the remaining 14 were not assigned to a domain. Thus the unit cell was well-determined. A full-sphere of intensity data was collected to a resolution of 0.49 Å. Refinement data is summarized in **Table 7.9**, and atomic coordinates, occupational and anisotropic and equivalent isotropic displacement parameters maybe found in **Table 7.10**.

Analysis of single crystalline X-ray diffraction data from the Bruker D8 Quest collected on the BaSrNF sample indicated a cubic cell with space group $Fd\bar{3}m$ and a lattice parameter larger than that of double cubic Sr_2NF (see Section 5.2). This immediately suggested an ordered rocksalt-type lattice for this phase. Interestingly, the final cell parameter here of a = 10.8637(9) Å is almost double the value of a = 5.4783(2) Å for the rocksalt-type BaSrNF phase discussed in the last section. That it is not quite doubled (or slightly more than doubled as seen in M_2NF systems) is due to the fact that it has a slightly smaller amount of Ba in the lattice relative to the BaSrNF disordered rocksalt-type phase, somewhat decreasing its relative lattice dimensions.

Table 7.9 Refinement data for ordered ordered rocksalt-type BaSrNF

Identification code	02022018_hoff
Empirical formula	BaSrNF
Formula weight	257.97
Temperature	100(2) K
Wavelength	0.71073 Å
Crystal system	Cubic
Space group	$Fd\bar{3}m$
Unit cell dimensions	a = 10.8637(9) Å
Volume	1282.1(3) $Å^3$
Z	16
Density (calculated)	5.346 Mg/m^3
Absorption coefficient	28.604 mm^{-1}
F(000)	1760.0
Crystal size	0.06 × 0.118 × 0.197 mm^3
Theta range for data collection	5.309 to 57.652°.
Index ranges	-24<=h<=12, -24<=k<=25, -25<=l<=25
Reflections collected	9301
Independent reflections	475 [R(int) = 0.0620]
Completeness to theta = 25.242°	95.9%
Absorption correction	Multi-scan
Refinement method	Full-matrix least-squares on F^2
Data / restraints / parameters	475 / 2 / 16
Goodness-of-fit on F^2	1.245
Final R indices [I>2sigma(I)]	$R1(F)^a$ = 0.0429, $wR2(F^2)^b$ = 0.0927
R indices (all data)	$R1(F)^a$ = 0.0510, $wR2(F^2)^b$ = 0.1017
Extinction coefficient	n/a
Largest diff. peak and hole	2.792 and -1.509 $eÅ^{-3}$

$^aR_1(F) = \Sigma \left| \left| F_o \right| - \left| F_c \right| \right| / \Sigma \left| F_o \right|$ with $F_o > 4.0\sigma(F)$. $^bwR_2(F^2) = [\Sigma[w(F_o^2 - F_c^2)^2]/\Sigma[w(F_o^2)^2]]^{1/2}$ with $F_o > 4.0\sigma(F)$, and $w^{-1} = \sigma^2(F_o)^2 + (W \cdot P)^2 + T \cdot P$, where $P = (Max(F_o^2,0) + 2F_c^2)/3$, W = 0.0235 , and T = 21.20

Table 7.10 Atomic coordinates (x 10^4), occupational, and *anisotropic and equivalent isotropic displacement parameters (Å^2 x 10^3) for ordered rocksalt-type BaSrNF.

Atom	$Fd\bar{3}m$ (No. 227) Wyc-koff Site	Refined Occ. Factor	No. of Atoms/ Unit Cell	X	Y	Z	U^{11}	U^{23}	U(eq)
Ba1	32e	0.351(3)	11.232(96)	83(1)	2417(1)	83(1)	8(1)	0(1)	8(1)
Sr1	32e	0.649(3)	20.768(96)	10(1)	2490(1)	83(1)	28(1)	2(1)	28(1)
F1	16d	0.9748(2)	15.597(3)	0	5000	0	26(1)	8(1)	26(1)
F2	8a	0.1726(4)	1.381(3)	1250	6250	1250	90(50)	0	90(50)
N1	16c	0.96927(7)	15.508(1)	0	0	0	11(1)	-1(1)	11(1)
F3	16c	0.03088(11)	0.494(2)	0	0	0	11(1)	-1(1)	11(1)

*The anisotropic thermal parameter is expressed as exp [$-2\pi^2(h^2 a^{*2} U_{11} + k^2 b^{*2} U_{22} + l c^{*2} U_{33} + 2hka^*b^*U_{12} + 2 hla^*b^*U_{13} + 2klb^* c^* U_{23})$]; $U_{11} = U_{22} = U_{33}$ and $U_{23} = U_{13} = U_{12}$ for all atoms. U(eq) is defined as one-third of the trace of the Uij orthogonalized tensor. N(1) and F(3) share the 16c site, displacement parameters constrained to be equal.

Experimental compositional analysis using the EDS method in a FIB/SEM (see Section 4.2) was attempted on the BaSrNF crystal subjected to X-ray diffraction analysis described in this section. Unfortunately, the crystal was very small and was completely decomposed by the time it was transported to the electron microscopy facility adjacent to the X-ray lab. A larger crystal ($1.35 \times 0.18 \times 0.14$ mm^3) from another reaction mixture (but with identical preparation route) was instead analyzed, after being verified on the diffractometer as having a doubled cubic lattice (unit cell parameter a =10.8295(4) Å). Figure 7.6 shows the resulting data, which indicates that a large amount of oxygen was

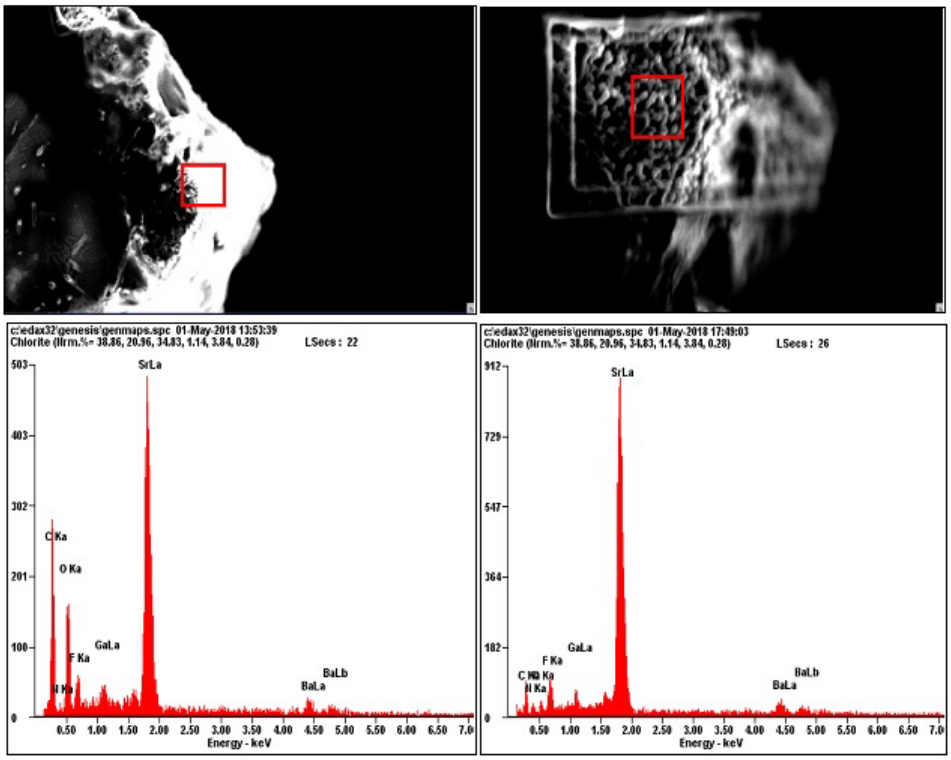

Element	Wt%	At%
CK	41.09	66.61
NK	01.62	02.25
OK	15.32	18.65
FK	04.30	04.41
GaL	02.38	00.66
SrL	30.05	06.68
BaL	05.24	00.74
Matrix	Correction	ZAF

Element	Wt%	At%
CK	18.23	49.00
NK	05.02	11.57
OK	02.18	04.39
FK	06.32	10.73
GaL	02.34	01.08
SrL	57.89	21.33
BaL	08.03	01.89
Matrix	Correction	ZAF

Figure 7.6. Focused ion beam (FIB) images and EDXS data of BaSrNF (different preparation from doubled cubic BaSrNF sample characterized via X-ray diffraction in this work). Carbon content is likely from the mineral oil used to protect the sample during the crystal selection process; gallium atoms are due to the focused ion beam used to mill away surface layers. **Left**: Data from the surface shows presence of oxygen; **Right**: data from crystal core, a significant reduction of oxygen is observed.

observed on the surface, while a much smaller amount was observed at the core. This strongly suggests that surface exposure to moisture during transport of the crystal to the SEM has occurred, with the BaSrNF phase likely reacting with water to form ammonia, metal hydroxides and metal fluorides as we have often observed in lab for M_2NF compounds (M = Ca, Sr, or Ba).

It is not possible here to determine whether or not the presence of oxygen at the core was present initially, or formed from decomposition. Taking the atomic percentages of Ba, Sr, N, O, and F at the core as comprising 100% by atoms in the sample gives a qualitative empirical composition of $Ba_{0.038}Sr_{0.43}N_{0.23}O_{0.088}F_{0.21}$, or almost 9% oxygen in the sample, with an undeterminable amount of this possibly due to decomposition. As this was a different sample from a separate preparation than the one refined here, and as oxygen does not affect the refinement model, it was not included in this refinement. At best, these results permit us to conclude that decomposition has occurred at least on the sample surface for the crystal analyzed. To check for possible decomposition during X-ray data collection in the sample refined here, a unit cell determination was done using reflections from the final frames of data collected. All reflections fit the initial unit cell with no evidence of decomposition present.

Figure 7.7 shows a unit cell plot for BaSrNF in which the characteristic ordering of N^{3-} and F^- ions along [100] for the doubled cubic phase is evident. It is also seen that there are three fluorine positions, including the F2 interstitial site which is is partially filled, as we have always observed so far in studies of ordered rocksalt-type phases. The refined composition (see Table 7.10) is $Ba_{0.70}Sr_{1.30}N_{0.97}F_{1.09}$ relative to the ideal M_2NF formula, or $Ba_{11.23}Sr_{20.77}N_{15.51}F_{17.47}$ per unit cell. From these refined compositions,

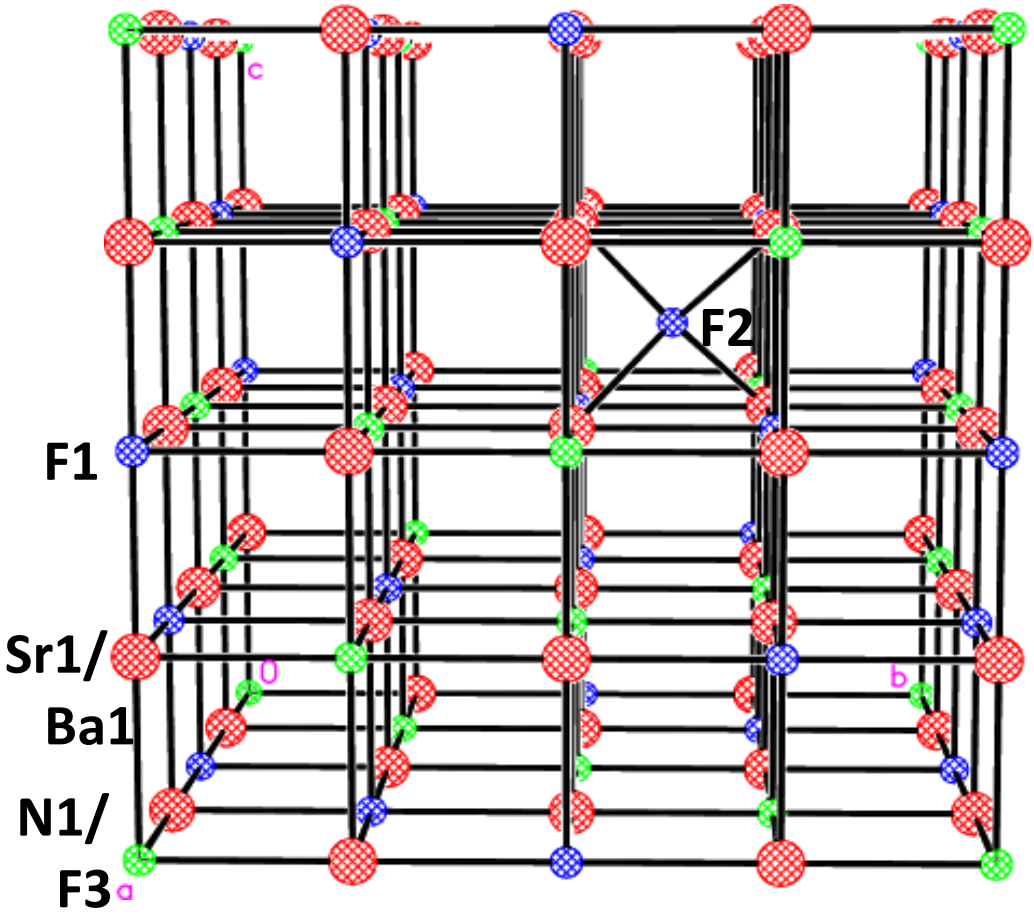

Figure 7.7. BaSrNF unit cell, ordered rocksalt phase, a =10.8637(9) Å. One filled F2 interstitial site shown, very little disorder at the F1 octahedral position was observed in this structure. Ba & F3 atoms not shown.

showing an excess of F^- ions and a deficiency of N^{3-} ions, it is evident that the model here predicts a non-stoichiometric defect as observed for Sr_2NF in this study (see Chapter 5), or in Ca_2NF by Al-Azzawi *et al*. (2017). However from the site-specific refined composition of $Ba_{11.23}Sr_{20.77}(N1_{15.51}\,F3_{0.49})F1_{15.60}F2_{138}$, it is seen that unlike the Ca_2NF and Sr_2NF phases just mentioned, there are 0.40 vacancies at the F1 octahedral position in the model. Thus, in addition to a non-stoichiometric defect, some of the F^- ions at the interstitial F2 site are due to a Frenkel defect with displacement of F1 atoms to F2 positions. The large thermal displacement at the F2 site visible in **Figures 7.8 & 7.9** is likely due to movement of F2 atoms closer to nearby F1 sites when they are vacant.

Further disorder in the model occurs at the Ba/Sr site, in which it was found that refining the positions and anisotropic displacement parameters separately decreased R values significantly from R1/wR2 = 0.1550/0.2973 (all data) to . R1/wR2 = 0.0786/0.2385 (all data). The Ba and Sr atoms are 0.141 Å apart. **Figure 7.8** shows the local Sr/Ba environment.

Figure 7.9 shows the local coordination environment of the F2 interstitial position. Comparison to Figure 5.3 shows that this is very different from the local F2 environment in Sr_2NF, where splitting of F1 into F1A positions 0.564 Å on either side of F1 occurs as a way to increase the short F2 – F1 distance of 2.310 Å. For the BaSrNF crystal, relatively little disorder occurs at the F1 positon. This may be due to a somewhat larger cell parameter compared to Sr_2NF (10.8637(9) Å vs. 10.6729(3) Å), opening up the lattice and relaxing the F2-F1 repulsions.

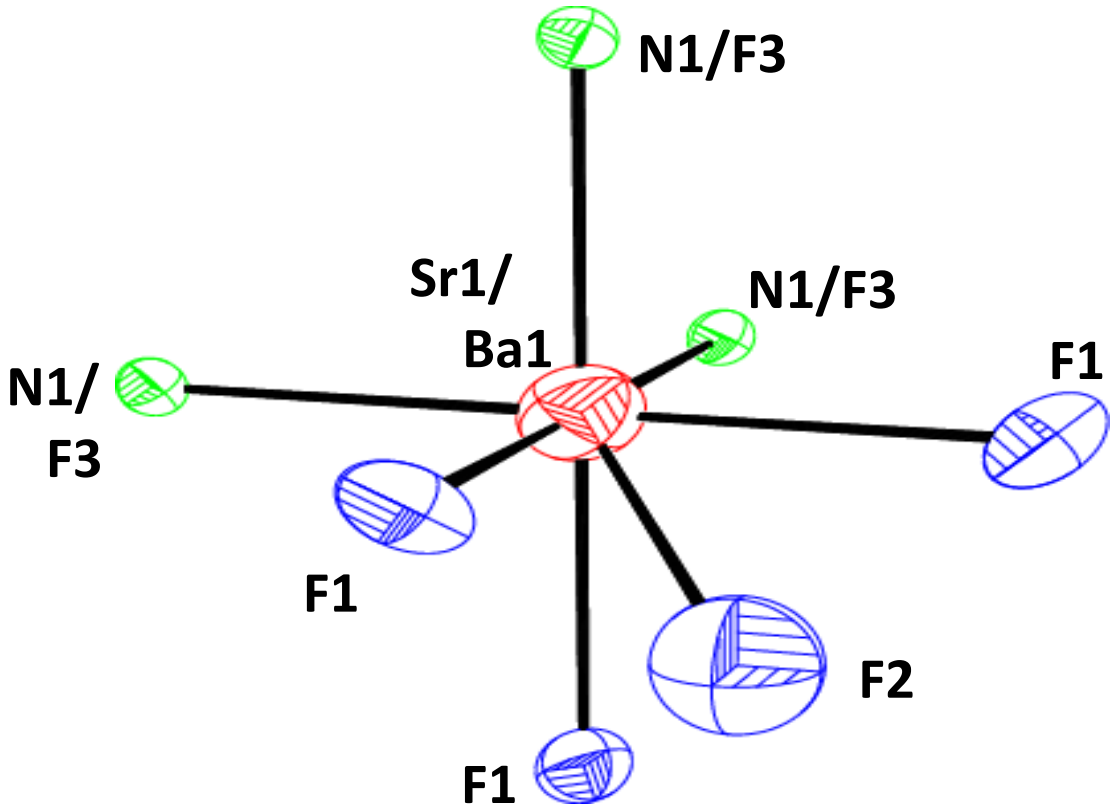

Figure 7.8. Local environment of Sr1/Ba1 in BaSrNF, ordered rocksalt phase, a = 10.8637(9) Å. The Sr1 and Ba1 atoms are 0.141 Å apart. Minimal disorder at F1 evident relative to Sr_2NF (Figure 5.3). 75% ellipsoids.

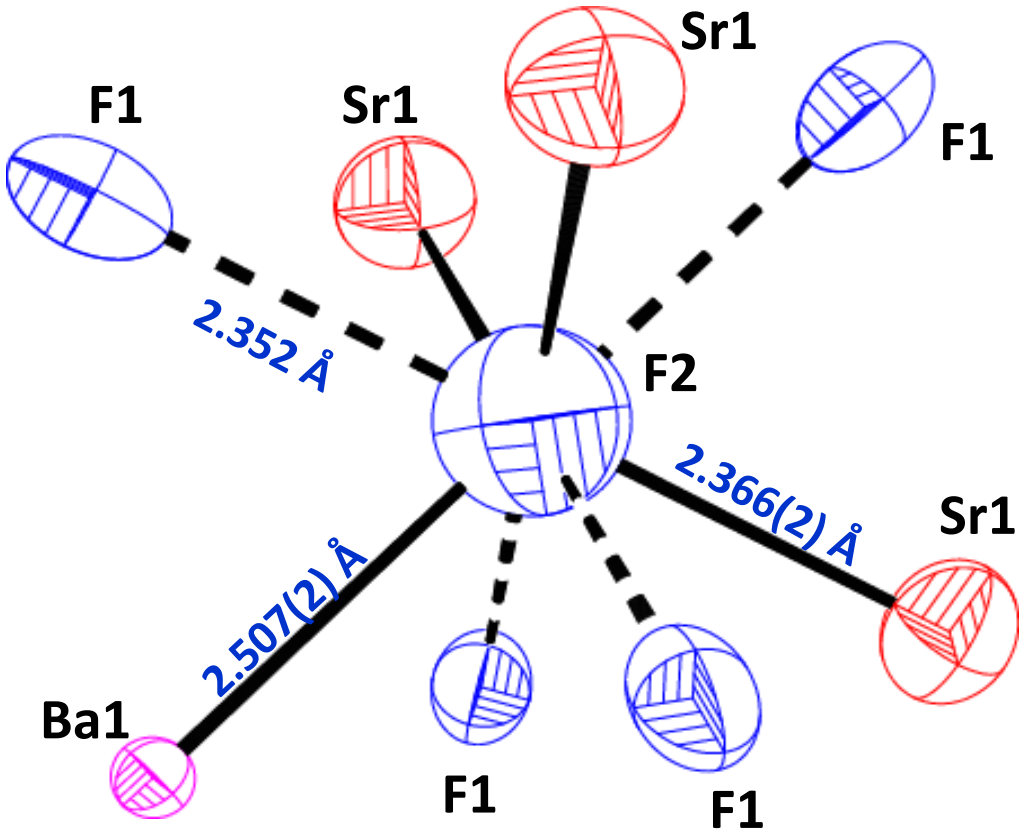

Figure 7.9. Local environment of F2 in BaSrNF, ordered rocksalt phase, a = 10.8637(9) Å. The shared Sr/Ba position refined to a Ba:Sr occupancy of 0.35:0.65; sites in the figure are arbitrarily labeled as either Sr or Ba. The slightly longer F2 to F1 distance of 2.352 Å here vs. 2.310 Å in Sr_2NF accounts somewhat for less disorder observed here at the F1site. The fairly large displacement of F2 may reflect a tendency for F2 atoms to move closer to the F1 position when that site is vacant (see text). 75% ellipsoids.

7.4 Conclusions

Two bimetallic Group II nitride fluoride composition systems were studied in this work – Ba-Ca-N-F and Ba-Sr-N-F. Preparation of single crystalline inorganic nitride fluorides from the melt typically yields a range of compositions and phases, and in this project two Ba-rich BaCaNF phases and two Sr-rich BaSrNF were prepared and characterized. Like all M_2NF compounds containing one Group II metal, both systems yielded samples crystallizing with the disordered rocksalt-type structure. In addition, both systems showed crystal chemistries that paralleled that of the metal-rich M_2NF system, as might be expected. Thus Ba-rich BaCaNF has the layered rhombohedral structure like Ba_2NF, and Sr-rich BaSrNF has the doubled cubic structure, but with less disorder than seen in Sr_2NF. Control of ratios of mixed metals in nitride fluorides, e.g. through powder synthesis, would add a dimension of diversity of crystal chemistry, and optical & electronic properties already present through N-F anion composition alone.

CHAPTER EIGHT

SUMMARY AND FUTURE WORK

The project focused mainly on the synthesis and characterization of bimetallic Group II nitride fluorides of ideal composition BaMNF (M = Mg, Ca, Sr), however a single crystal study on Sr_2NF was also revisited. Four new bimetallic Group II nitride fluoride compounds were successfully prepared and characterized in this study. Metal nitride fluoride compounds are highly sensitive to air and moisture contamination, and thus the procedures were focused to minimize the exposure to air to achieve phase purity. The preparation method involved cooling a mixture of metal and metal fluorides from the melt at high temperature under nitrogen. Under these conditions, the compositions and phases of the single crystalline samples obtained depend on which are the most stable phases, and possibly on local composition during growth of specific crystals. While the phases and exact compositions were not controlled, the samples obtained gave deep insight into the crystal chemistries of the Group II bimetallic N-F systems studied. No bimetallic Group II nitride fluoride compounds have previously been reported.

Two new compounds in the Ba-Ca-N-F system were prepared and characterized. They are both Ba-rich, and not surprisingly exhibit very similar crystal chemistry to Ba_2NF. One of the new compounds has a disordered rocksalt-type structure (a = 5.5361(15) Å) with refined composition $Ba_{1.66}Ca_{0.34}NF$, while the other has the layered rhombohedral structure (a = 3.9646(3) Å, c = 19.7792(17) Å) with refined composition $Ba_{1.82}Ca_{0.18}NF$. To our knowledge, the latter compound is the first single crystal study of a layered rhombohedral N-F compound. This structure consists of $[M_2N]^+$ layers separated by X^- (halide ion) layers. If the $[M_2N]^+$ layers are not a minimum distance

apart (around 3.5 Å), repulsion between these charged layers instead drives crystallization to either the ordered (i.e. doubled cubic) or disordered rocksalt-type phases, neither of which are layered.

For M_2NX compounds with larger halide ions (i.e. X = Cl^- or Br^-) or for a large metal ion, the layered phase is favored. Ba_2NF is the only M_2NF compound that has the layered structure, and this phase has never been observed to form the ordered rocksalt phase. On the other hand, $Ca_2NF$and Sr_2NF, which would have interlayer spacing of only around 3 Å (Bailey *et al*., 2011), have never been observed has having the layered rhombohedral structure. Interestingly, our compound, in which some Ca^{2+} ions replace larger Ba^{2+} ions has a larger M_2N^+ interlayer spacing compared to Ba_2NF, possibly due to distortion of the $N(Ba_{5.46}Ca_{0.54})$ octahedra.

The two new phases in the Ba-Sr-N-F system that were prepared and characterized in this work are both Sr-rich, and reflect a crystal chemistry very close to Sr_2NF with both disordered and ordered rocksalt-type phases observed. The refined compositions are $Ba_{0.82}Sr_{1.18}NF$ for the disordered rocksalt (a = 5.4783(2) Å), and $Ba_{0.70}Sr_{1.30}N_{0.97}F_{1.09}$ for the ordered rocksalt (a = 10.8637(9) Å). Unlike ordered rocksalt-type Sr_2NF, which was found in this work to have a non-stoichiometric defect with significant disorder at the F1 octahedral site, the analogous BaSrNF phase showed relatively little disorder at the F1 site. In Sr_2NF (a = 10.6729(3) Å), the nearby F2 interstitial atoms cause the F1 atoms to shift away from F2 to increase the distance between them. For the BaSrNF doubled cubic phase, the larger lattice apparently relaxes the F2-F1 repulsion, and so the F1 position is not shifted.

Attempted syntheses of BaMgNF phases in this work were not successful, as either metal nitrides, magnesium nitride fluorides, and/or barium nitride fluoride phases preferentially formed via our synthesis route. Future attempts will be made to prepare mixed metal Ba-Mg-N-F phases. The relatively large difference in sizes of Ba^{2+} vs. Mg^{2+} (Ba/Mg size ratio = 2.37 vs. 1.35 for Ba/Ca) means that these atoms would likely occupy separate lattice sites rather than sharing a position, which could open up a new class of Group II inorganic nitride-fluoride compounds.

Compositional analysis was done via EDS analysis on the Sr_2NF crystal ran in the X-ray diffractometer for this work, and on a BaSrNF crystal verified as a doubled cubic phase, although not the same one reported here. In both cases the compositional data showed the presence of oxygen on the surface and much smaller amounts in the core of the crystal. Crystal decomposition at the surface therefore occurred by the time compositional analysis began, but it is not possible to say whether or not oxygen at the crystal core was due to decomposition, or oxygen impurity incorporated during the reaction, or both. Due to the fact that the amounts of oxygen detected at the crystal cores were relatively small and would likely have little effect on the crystal refinements and refinement models, oxygen was ignored during the refinements. This was tested for Sr_2NF, where substituting O atoms for F atoms at the F3 site made little difference in the refinement, except for slightly poorer R values. Future work is required to resynthesize these phases and verify phase purity.

Future work will also include computational modeling of band gaps from our known structures. This will verify if band gaps decrease as N content increases in M_2NF phases, and also to what extent band gaps can be tuned by metal substitution in

compounds such as the BaMNF (M = Ca, Sr) mixed metal phases synthesized in this work.

REFERENCES

Al-Azzawi, M. (2016). MS Thesis: Synthesis and Characterization of Single Crystalline Metal Nitride Fluorides, Youngstown State University.

Al-Azzawi M., Zeller M., Li, D., Wagner T. (2017). Crystal chemistry of ordered rocksalt-type Ca_2NF. *J. of Solid State Chem*., **254**, 126-131.

Andersson, S. (1970). Magnesium nitride fluorides. Journal of Solid State Chemistry, **1**(3-4), 306-309. doi:10.1016/0022-4596(70)90109-x

Bailey, A. S., Hughes, R. W., Hubberstey, P., Ritter, C., Smith, R. I., & Gregory, D. H. (2011). New ternary and quaternary barium nitride halides; synthesis and crystal chemistry. *Inorg. Chem*., **50**(19), 9545-9553. doi:10.1021/ic201264u

Brese, N.E., O'Keeffe, M. (1991). Bond-Valence Parameters for Solids. *Acta Cryst*., **B47**, 192-197.

Brogan, M. A., Hughes, R. W., Smith, R. I., & Gregory, D. H. (2012). Structural studies of magnesium nitride fluorides by powder neutron diffraction. Journal of Solid State Chemistry, **185**, 213-218. doi:10.1016/j.jssc.2011.11.008

Ehrlich, P., Linz, W, Seifert, H. (1971).Nitrofluoride der Schweren Erdalkalimetalle. Naturwisenschanften **58**,219-220.

Fang, C.M., Ramanujachary, K.V., Hintzen, H.T., de With, G. (2003). Electronic structure of magnesium nitride-fluorides from first-principles calculations. J. of Alloys and Compounds, **351**, 72-76.

Keino, M.S (2017). Investigations of mixed analogs of Manganite Perovskites and Bimetallic Group II Nitride Fluorides. MS Thesis, Youngstown State University.

Galy, J. Jaccou, M. and Andersson, S. (1971). Nitrofluoride, Ca_2NF.oxynitrofluorinated solid solutions $Ca_2O_{2x}N1_{-x}$ $F1_{-x}$,C.R. Acad. Sc. Paris, **272**, 1657

Headspith, D. A., Sullivan, E., Greaves, C., & Francesconi, M. G. (2009). Synthesis and characterization of the quaternary nitride-fluoride $Ce_2MnN_3F_2{-}\delta$. Dalton Transactions Dalton Trans., **42**, 9273. doi:10.1039/b908591b

Jack, D. R., Zeller, M., & Wagner, T. R. (2005). Doubled-Cubic Ca_2NF. ChemInform, **36(14)**. doi:10.1002/chin.200514011

Nicklow, R.A., T.R. Wagner, and C.C. Raymond (2001). Preparation and Single-Crystal Structure Analysis of Ca_2NF. Journal of Solid State Chemistry: **160**, 134-38.

Seibel, H., and T.R. Wagner (2004). Preparation and Crystal Structure of Ba_2NF. Journal of Solid State Chemistry: **177**, 2772-776.

Sheldrick, G.M. (2008). , Acta Cryst.: **A64**, 112-122.

Stoltz, C., Ramesha, K., Piccoli, P., Toby, B. H., & Eichhorn, B. W. (2005). $A_{0.3}ZrNF_{1.3}$ Phases (A = Na, K) with layered ZrNCl-type structures prepared by anion metathesis. Chemistry of Materials Chem. Mater.: **17(21)**, 5291-5296. doi:10.1021/cm051018h

Strozewski, M. S. (2007). Synthesis and crystal chemistry of $Ca_2N_xO_{2-2x}F_x$ (x = 0 to 1) and other compounds. MS Thesis, Youngstown State University.

Wagner, T. (2002). Preparation and single-crystal structure analysis of Sr_2NF. Journal of Solid State Chemistry: **169**, 13-18.